

# BMJ Open Genome-wide association study of perioperative myocardial infarction after coronary artery bypass surgery

Miklos D Kertai,<sup>1</sup> Yi-Ju Li,<sup>2,3</sup> Yen-Wei Li,<sup>2</sup> Yunqi Ji,<sup>2</sup> John Alexander,<sup>4,5</sup> Mark F Newman,<sup>1,5</sup> Peter K Smith,<sup>6</sup> Diane Joseph,<sup>5</sup> Joseph P Mathew,<sup>1</sup> Mihai V Podgoreanu,<sup>1,5</sup> for the Duke Perioperative Genetics and Safety Outcomes (PEGASUS) Investigative Team

**To cite:** Kertai MD, Li Y-J, Li Y-W, *et al.* Genome-wide association study of perioperative myocardial infarction after coronary artery bypass surgery. *BMJ Open* 2015;5:e006920. doi:10.1136/bmjopen-2014-006920

► Prepublication history and supplementary files are available. To view please visit the journal (<http://dx.doi.org/10.1136/bmjopen-2014-006920>).

Received 14 October 2014  
Revised 10 March 2015  
Accepted 12 March 2015

## ABSTRACT

**Objectives:** Identification of patient subpopulations susceptible to develop myocardial infarction (MI) or, conversely, those displaying either intrinsic cardioprotective phenotypes or highly responsive to protective interventions remain high-priority knowledge gaps. We sought to identify novel common genetic variants associated with perioperative MI in patients undergoing coronary artery bypass grafting using genome-wide association methodology.

**Setting:** 107 secondary and tertiary cardiac surgery centres across the USA.

**Participants:** We conducted a stage I genome-wide association study (GWAS) in 1433 ethnically diverse patients of both genders (112 cases/1321 controls) from the Genetics of Myocardial Adverse Outcomes and Graft Failure (GeneMAGIC) study, and a stage II analysis in an expanded population of 2055 patients (225 cases/1830 controls) combined from the GeneMAGIC and Duke Perioperative Genetics and Safety Outcomes (PEGASUS) studies. Patients undergoing primary non-emergent coronary bypass grafting were included.

### Primary and secondary outcome measures:

The primary outcome variable was perioperative MI, defined as creatine kinase MB isoenzyme (CK-MB) values  $\geq 10\times$  upper limit of normal during the first postoperative day, and not attributable to preoperative MI. Secondary outcomes included postoperative CK-MB as a quantitative trait, or a dichotomised phenotype based on extreme quartiles of the CK-MB distribution.

**Results:** Following quality control and adjustment for clinical covariates, we identified 521 single nucleotide polymorphisms in the stage I GWAS analysis. Among these, 8 common variants in 3 genes or intergenic regions met  $p < 10^{-5}$  in stage II. A secondary analysis using CK-MB as a quantitative trait (minimum  $p = 1.26 \times 10^{-3}$  for rs609418), or a dichotomised phenotype based on extreme CK-MB values (minimum  $p = 7.72 \times 10^{-6}$  for rs4834703) supported these findings. Pathway analysis revealed that genes harbouring top-scoring variants cluster in pathways of biological relevance to extracellular matrix remodelling, endoplasmic reticulum-to-Golgi transport and inflammation.

## Strengths and limitations of this study

- This is the first genome-wide association study of perioperative myocardial infarction, using prospective cohorts of cardiac surgical patients, standard definitions of the primary phenotype and full adjustment for non-genetic risk factors.
- We conducted comprehensive and complementary single marker and pathway-based genome-wide association analyses.
- The study is powered to detect relatively large effect sizes.
- Rare genetic variant effects not analysed.
- Predominantly Caucasian cohort, thus findings cannot be generalised to other populations.

**Conclusions:** Using a two-stage GWAS and pathway analysis, we identified and prioritised several potential susceptibility loci for perioperative MI.

## INTRODUCTION

Despite advances in surgical techniques and pharmacological therapy, the incidence of myocardial infarction (MI) after coronary artery bypass grafting (CABG) remains as high as 19%, and is associated with increased mortality and long-term morbidity.<sup>1</sup> Strategies to identify subpopulations of patients at risk for developing large myocardial infarcts on the one hand, or those displaying an intrinsic cardioprotective state on the other hand, remain high-priority knowledge gaps and could inform selection of more specific protective agents.<sup>2</sup>

The evidence for heritability of MI is striking, supported both by family studies and, recently, by a number of well powered and replicated genome-wide association studies (GWAS), which primarily implicate common genetic variants at the 9p21 locus in multiple racial groups.<sup>3–6</sup> However, although family-



CrossMark

For numbered affiliations see end of article.

### Correspondence to

Dr Mihai V Podgoreanu;  
mihai.podgoreanu@duke.edu

based methods are not practical for studying perioperative MI (PMI), its genetic basis is strongly suggested by several observations, including wide variability in incidence and severity that is poorly explained by clinical and procedural risk factors, different racial susceptibility profiles and results from preclinical animal models. Indeed, extensive genetic variability has been found in biological pathways implicated in the pathophysiology of postoperative MI, such as the complex acute inflammatory response to cardiac surgery. Mounting evidence for heritability of a proinflammatory state suggests that individual genetic history may also significantly modulate the magnitude of postoperative inflammatory response after cardiac surgery.<sup>7</sup> Yet only a few studies have identified allelic associations with altered susceptibility to myocardial ischaemia-reperfusion injury in cardiac surgical populations, all based on a candidate gene association approach.<sup>8–12</sup> Thus, the overall influence of common genetic variation on the incidence of PMI remains poorly understood.

Recently, integrated testing of genes involved in the same biological pathway has emerged as an alternative strategy for evaluating the combined effects of multiple genetic variants with small effect size on a disease phenotype.<sup>13–15</sup> Given the polygenic nature of disease susceptibility, this approach is increasingly being used to identify groups of gene variants with shared cellular function that are enriched for disease, while also improving the statistical power of GWAS. In this study, we adopted this strategy by first employing genome-wide association methodology to identify common genetic variants associated with PMI after CABG, followed by pathway-based analyses to uncover biological mechanisms of relevance to PMI.

## METHODS

The study design and reporting of the results follow the recommendations by 'Strengthening the Reporting of Genetic Association Studies' (STREGA).<sup>16</sup> We performed a joint two-stage<sup>17</sup> GWAS combined with a pathway analysis approach.

### Patient populations

The stage I cohort (discovery cohort) comprised 1493 ethnically diverse subjects who underwent an isolated CABG with cardiopulmonary bypass for the first time and were enrolled between 2002 and 2003 in the Institutional Review Board (IRB) approved Genetics of Myocardial Outcomes and Graft Failure (GeneMAGIC) ancillary substudy of the multicentre Project of Ex-vivo Vein Graft Engineering via Transfection (PREVENT-IV).<sup>18</sup> Of those, 1433 patients met eligibility requirements after applying quality control criteria and excluding patients with missing genotypes or phenotypic information.

In stage II, we tested the top genetic variants in an expanded data set in which an additional 622 patients of self-reported European ancestry were added to the

discovery data set, leading to a total of 2055 patients. The additional patients underwent CABG with cardiopulmonary bypass between 1997 and 2006 as part of the Perioperative Genetics and Safety Outcomes Study, an IRB-approved longitudinal study at the Duke University Medical Center.<sup>11 12</sup>

### Definition of PMI

PMI was defined according to the universal definition of MI<sup>19</sup> as an elevation in the plasma level of creatine kinase MB isoenzyme (CK-MB) that was >10 times the upper limit of normal, as measured by a core laboratory within 24 h after surgery, and that was not attributable to an intervening clinical event or preoperative MI (adjudicated by the PREVENT-IV Clinical Events Committee).<sup>18</sup>

### Genotyping and quality controls

Genomic DNA was isolated from whole blood or saliva using standard procedures. Genotyping in both cohorts was performed on the Illumina Human610-Quad BeadChip at the Duke Genomic Analysis Facility. Sample and genotype quality control of data flow included assessment of call rates, gender check, cryptic relatedness, SNP missingness and the Hardy-Weinberg equilibrium, as previously described.<sup>20</sup> We used principal components derived from the EIGENSTRAT<sup>21</sup> method to control for population stratification (see online supplementary methods).

### Statistical analysis

Univariate regression analysis was performed to test differences in demographic, clinical and procedural characteristics between patients with and without postoperative MI; statistically significant covariates were subsequently used to adjust genetic association tests. Genome-wide association analyses performed in the stage I cohort used multivariable logistic regression models implemented in PLINK 1.07, assuming an additive genetic model, and including significant clinical covariates and the top 10 principal components to adjust for population stratification (see online supplementary table S1). Statistical significance for stage I analyses was a priori arbitrarily defined as a two-tailed  $p < 0.001$ , to balance between the overly conservative Bonferroni correction and type II error, given that we had an a priori defined replication data set to obviate type I error. In stage II analyses, the same clinical covariate and principal component adjustments (re-estimated for the expanded data set) were applied, with statistical significance defined as a Bonferroni adjusted  $p$  value of 0.05/number of SNPs identified in stage I, to control the overall type I error rate. Haplotype association analysis was performed in the stage II cohort for genes tagged by the significant SNPs, adjusting for the same clinical covariates and principal components. Secondary analyses were performed for the top SNPs identified in the stage II cohort, using the continuous phenotype of CK-MB values and a dichotomised extreme CK-MB

phenotype, which included participants within the first and fourth quartiles of the CK-MB distribution. For CK-MB, a linear regression model was applied with adjustment for the same set of covariates as in the primary analysis. For the extreme CK-MB subset, we re-assigned trait status as '0' for participants within the first CK-MB quartile, and '1' for participants within the fourth CK-MB quartile from the stage II cohort. Logistic regression with the same set of covariates was performed. Finally, we employed pathway analysis to prioritise association results and provide biological interpretation, using functional ontology enrichment analysis tools implemented in MetaCore (GeneGO, St. Joseph, MI; see online supplementary methods).

## RESULTS

PMI was observed in 112 of 1433 patients (7.8%) and in 225 of 2055 patients (10.9%) in stage I and II cohorts, respectively (see online supplementary table S2). Aortic cross-clamp time, number of coronary artery grafts, and procedures in addition to CABG were significantly associated with PMI in stage I analyses. Stage II analyses showed that extracardiac arteriopathy and year of surgery also played significant roles. All the clinical variables identified above were included in multivariable logistic regression models to adjust the genetic association tests for potential confounders (see online supplementary table S2).

After applying quality control criteria (see online supplementary methods: A.1. Quality control of data flow), 534 390 markers were analysed for association with PMI in stage I. While none of the SNPs reached genome-wide significance (figure 1), 521 SNPs met the a priori defined discovery threshold of  $p < 0.001$  (minimum  $p = 2.76 \times 10^{-6}$ , rs2044061 on chromosome 8) and were subsequently analysed in stage II (see online supplementary table S10). A quantile-quantile (Q-Q) plot of

observed versus expected p values showed that the population substructure was well adjusted for (see online supplementary figure S2).

In stage II analyses, eight of the 521 SNPs met the Bonferroni correction threshold ( $p < 9.6 \times 10^{-5}$  for 521 SNPs). The top 2 SNPs (rs10454444 and rs10913237), located in the pregnancy-associated plasma protein A2 gene (*PAPPA2*), were in high linkage disequilibrium, with p values for stage II of  $2.43 \times 10^{-6}$  (OR 0.46; 95% CI 0.33 to 0.63) and  $2.47 \times 10^{-6}$  (OR 0.46; 95% CI 0.33 to 0.63), respectively. In addition, one intronic SNP in histone deacetylase-4 (*HDAC4*), two in the SEC24 family, member D (*SEC24D*, a member of the cytoplasmic coat protein complex II, COPII), and two located in intergenic regions were associated with PMI (table 1).

When CK-MB was tested as a quantitative trait, all eight SNPs remained significantly associated with plasma levels of CK-MB. However, rs4834703 in *SEC24D* ( $p = 7.72 \times 10^{-6}$ ) and rs10200850 in *HDAC4* ( $p = 8.26 \times 10^{-5}$ ) showed the strongest association, followed by the 2 SNPs in *PAPPA2* ( $p = 0.0001$ ; table 2). When the dichotomised extreme CK-MB phenotype was studied in the stage II cohort, only the 2 SNPs located in *SEC24D* (rs4834703 and rs6822035,  $p = 0.002$ ) and rs609418 in the intergenic region between *RFXAP* and *SMAD9* ( $p = 0.001$ ) remained nominally significant (table 2). Overall, the rs4834703 SNP in *SEC24D* consistently showed strong association signals across postoperative MI, quantitative CK-MB and the extreme CK-MB traits.

The haplotype structures of genic regions surrounding the significant SNPs in *PAPPA2*, *HDAC4* and *SEC24D* are shown in online supplementary figure S3, and the results of haplotype analysis are shown in table 3 and online supplemental table S3. Haplotype analysis performed for the linkage disequilibrium blocks containing the significant markers showed that the A-A haplotype (rs6822035, rs10518325) in *SEC24D* had the most

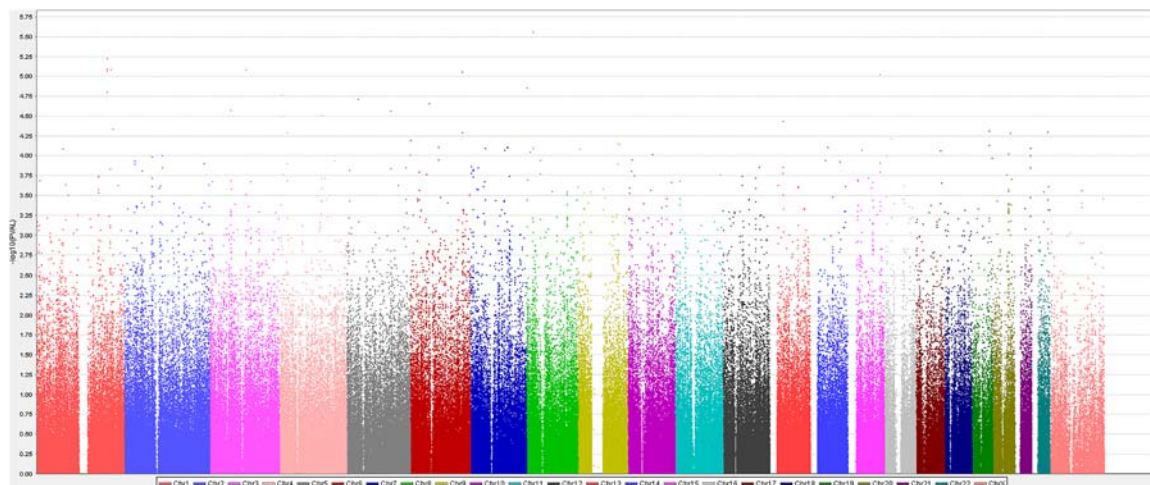


**Figure 1** Manhattan plot of genome-wide association with perioperative myocardial infarction in stage I analysis. The x axis represents the genome in physical order (coloured by chromosome); the y axis showing  $-\log_{10}(p)$  for all single nucleotide polymorphisms (SNPs). None of the SNPs reached genome-wide significance ( $p < 9.09 \times 10^{-8}$ ), but 521 SNPs met the prespecified discovery threshold  $p < 0.001$  for inclusion in stage II analyses (minimum  $p = 2.76 \times 10^{-6}$ , rs2044061 on chromosome 8).

Table 1 Top eight SNP associated with postoperative myocardial infarction

Chr	SNP	Base pair	Gene symbol	Stage I: discovery data set*				Stage II: expanded data set*			
				MAF		p Value	OR (95% CI)	MAF		p Value	OR (95% CI)
				Controls N=1321	Cases N=112			Controls N=1830	Cases N=225		
1	rs10489478	176 566 350	PAPPA2	0.18	0.09	2.67×10 <sup>-4</sup>	0.41 (0.25 to 0.66)	0.18	0.11	0.47 (0.34 to 0.65)	4.70×10 <sup>-6</sup>
1	rs10913237	176 630 416	PAPPA2	0.18	0.09	1.85×10 <sup>-4</sup>	0.39 (0.24 to 0.64)	0.19	0.11	0.46 (0.33 to 0.63)	2.47×10 <sup>-6</sup>
1	rs10454444	176 649 181	PAPPA2	0.18	0.09	1.81×10 <sup>-4</sup>	0.39 (0.24 to 0.64)	0.19	0.11	0.46 (0.33 to 0.63)	2.43×10 <sup>-6</sup>
2	rs10 200 850	240 234 901	HDAC4	0.06	0.13	4.34×10 <sup>-4</sup>	2.22 (1.42 to 3.46)	0.06	0.11	2.23 (1.57 to 3.17)	8.18×10 <sup>-6</sup>
4	rs4834703	119 691 624	SEC24D	0.09	0.18	3.13×10 <sup>-5</sup>	2.27 (1.54 to 3.34)	0.09	0.16	1.98 (1.47 to 2.66)	6.80×10 <sup>-6</sup>
4	rs6822035	119 710 421	SEC24D	0.29	0.40	2.59×10 <sup>-4</sup>	1.73 (1.29 to 2.33)	0.28	0.36	1.65 (1.32 to 2.05)	9.55×10 <sup>-6</sup>
12	rs2303970	74 471 340	TRHDE LOC552889	0.48	0.35	3.51×10 <sup>-4</sup>	0.58 (0.43 to 0.78)	0.48	0.36	0.62 (0.50 to 0.76)	8.89×10 <sup>-6</sup>
13	rs609418	37 417 427	RFXPAP   SMAD9	0.25	0.35	3.14×10 <sup>-4</sup>	1.73 (1.28 to 2.33)	0.25	0.33	1.67 (1.34 to 2.09)	5.81×10 <sup>-6</sup>

\*Adjusted for clinical characteristics including extracardiac arteriopathy, recent myocardial infarction, procedure other than CABG only, year of surgery, number of diseased vessels and aortic cross-clamp time.

HDAC4, histone deacetylase-4; PAPPA2, pregnancy-associated plasma protein A2; RFXAP, regulatory factor X-associated protein; SEC24D, SEC24-related protein D; SMAD9, mother against decapentaplegic homolog 9; TRHDE, thyrotropin-releasing hormone-degrading ectoenzyme; intergenic region is expressed by two flanking genes with 'I' in between. CABG, coronary artery bypass grafting; Chr, chromosome; MAF, minor allele frequency (based on the discovery data set); SNP, single nucleotide polymorphisms.

significant association with postoperative MI ( $p=5.54\times 10^{-7}$ , OR 1.87; 95% CI 1.46 to 2.39, table 3).

In multivariate risk factor-adjusted stage I and II analyses, we found no evidence for association between genetic variation at the 9p21 locus and incident postoperative MI, including the rs10116277 SNP previously associated with MI and mortality in non-surgical<sup>20</sup> and cardiac surgical<sup>8 9</sup> cohorts (see online supplementary figure S4).

The top 10 enriched pathway maps for the stage I analysis SNPs are shown in online supplementary figure S5. The most significant were 'Cell adhesion: extracellular matrix remodelling' and 'Cytoskeleton remodelling: TGF, WNT, and cytoskeletal remodelling' (enrichment  $p$  value= $1.9\times 10^{-8}$  and  $7.3\times 10^{-6}$ , respectively). The most significant canonical pathway maps in stage I and II comparative analyses were 'Immune response: NFAT signalling and leucocyte interaction' and 'Cell adhesion: extracellular matrix remodelling' ( $p=7.2\times 10^{-4}$  and  $1.1\times 10^{-3}$ , respectively; see online supplementary tables S4 and 5).

## DISCUSSION

We present the first report of a two-stage GWAS involving 225 PMI cases and 1830 controls. After accounting for clinical and procedural covariates, we identified eight significant SNPs mapped to three genes (*PAPPA2*, *HDAC4*, *SEC24D*) and two intergenic regions. The most significant association with PMI was exhibited by rs10454444 in *PAPPA2* ( $p=2.43\times 10^{-6}$ ) in single-marker analyses, by *SEC24D* A-A (rs6822035, rs10518325,  $p=5.54\times 10^{-7}$ ) in haplotype analyses, and by *SEC24D* SNPs in secondary analyses when CK-MB was evaluated as a quantitative trait (rs4834703,  $p=2.43\times 10^{-6}$ ) or as an extreme CK-MB phenotype (rs4834703 and rs6822035,  $p=0.002$ ).

Among these eight SNPs, rs4834703 in *SEC24D* showed the most consistently strong association with all three phenotypes evaluated in this study. The transport protein *SEC24D* is an integral component of cytoplasmic COPII transport machinery, a key player in vesicle trafficking of secretory proteins from the endoplasmic reticulum (ER) to the Golgi apparatus for delivery to downstream compartments. COPII is responsible for cargo sorting and vesicle morphogenesis, with roles in modulating ER exit, cell surface transport, lipid secretion and cholesterol biosynthesis, and function of G protein-coupled receptors. Conditions of ischaemia, oxidative injury or acute phase-response result in ER stress through accumulation of misfolded proteins, which leads to activation of the unfolded protein response (UPR) signalling pathway. If the protective mechanisms activated by the UPR are insufficient, cells die by apoptosis and autophagy. However, altered expression or function of SEC24 proteins could also explain ER trapping of misfolded proteins under conditions of ER stress,<sup>22 23</sup> with SEC24D being the only isoform implicated in extracellular matrix secretion.<sup>24</sup> Animal

**Table 2** Association of the top eight SNP with CK-MB as a quantitative trait and as an extreme phenotype in the joint analysis data set

Chr	SNP	Base pair	Gene symbol	MAF (Overall)	CK-MB as a quantitative trait*		CK-MB as an extreme phenotype*	
					$\beta$ -Coefficient	p Value	OR (95% CI)	p Value
1	rs10489478	176 566 350	<i>PAPPA2</i>	0.17	-5.40	$2.27 \times 10^{-4}$	0.77 (0.574 to 1.047)	0.1
1	rs10913237	176 630 416	<i>PAPPA2</i>	0.18	-5.58	$1.30 \times 10^{-4}$	0.78 (0.578 to 1.052)	0.1
1	rs10454444	176 649 181	<i>PAPPA2</i>	0.18	-5.59	$1.21 \times 10^{-4}$	0.77 (0.575 to 1.043)	0.09
2	rs10200850	240 234 901	<i>HDAC4</i>	0.07	9.26	$8.26 \times 10^{-5}$	1.49 (0.950 to 2.326)	0.08
4	rs4834703	119 691 624	<i>SEC24D</i>	0.10	8.54	$7.72 \times 10^{-6}$	1.82 (1.242 to 2.654)	0.002
4	rs6822035	119 710 421	<i>SEC24D</i>	0.30	4.42	$4.81 \times 10^{-4}$	1.48 (1.152 to 1.903)	0.002
12	rs2303970	74 471 340	<i>TRHDE</i>	0.47	-2.93	0.01	0.84 (0.669 to 1.047)	0.12
13	rs609418	37 417 427	<i>LOC552889</i> <i>RFXAP/SMAD9</i>	0.26	4.80	$2.26 \times 10^{-4}$	1.56 (1.189 to 2.034)	0.001

\*Adjusted for clinical characteristics including extracardiac arteriopathy, recent myocardial infarction, procedure other than CABG only, year of surgery, number of diseased vessels, and aortic cross-clamp time using either linear regression ( $\beta$ -coefficient) or logistic regression (OR, 95% CI) analyses.

*HDAC4*, histone deacetylase-4; *PAPPA2*, pregnancy-associated plasma protein A2; *RFXAP*, regulatory factor X-associated protein; *SEC24D*, SEC24-related protein D; *SMAD9*, mother against decapentaplegic homolog 9; *TRHDE*, thyrotropin-releasing hormone-degrading ectoenzyme.

CABG, coronary artery bypass grafting; Chr, chromosome; CK-MB, creatine kinase MB isoenzyme; MAF, minor allele frequency (based on the expanded data set); SNP, single nucleotide polymorphisms.

models of defects in *SEC24D* involve characteristic skeletal malformations, whereas its complete disruption results in early-embryonic lethality.<sup>25</sup> However, there are no reports of human diseases associated with genetic variation in *SEC24D*.

*PAPPA2* is a metalloproteinase that regulates local insulin-like growth factor (IGF) bioavailability by specifically cleaving IGF-binding protein 5 (IGFBP-5). In experimental models of myocardial ischaemia, IGFBP-5 inhibits both myocardial IGF-1, with implications for inflammation-linked angiogenesis and repair processes,<sup>26</sup> and IGF-2, limiting its cardioprotective effects following ischaemia reperfusion.<sup>27–28</sup> The related protein *PAPPA1* cleaves IGFBP-4 and is activated and released from vulnerable atherosclerotic plaques. *PAPPA1* has been extensively studied as a cardiovascular risk biomarker for the diagnosis and prognosis of acute

coronary syndrome;<sup>29–30</sup> however, the role of *PAPPA2* in cardiovascular biology has not been previously reported. Consistent with our single-marker analysis findings, the GWAS pathway analysis identified significant contributions of variants in other IGF system component genes, namely IGF-2 and the IGF-1 receptor (see online supplementary figure S6 and table S5).

*HDAC4*, a member of the HDAC family, mediates changes in the chromatin structure by removing acetyl groups from the core histones, resulting in transcriptional repression. *HDAC4* is highly expressed in the myocardium, where it plays an important role in the regulation of gene expression and is involved in myocardial cell cycle progression, differentiation and apoptosis.<sup>31</sup> Experimental HDAC inhibition is associated with a profound reduction in ischaemia-induced myocardial cell death,<sup>31</sup> by triggering preconditioning effects and

**Table 3** Estimated haplotype frequencies in the *SEC24D* gene and results of association tests with incidence of PMI in the stage II analysis cohort (n=2055)

SNP1	SNP2	Haplotype	Haplotype frequency		OR (95% CI)	p Value
			Patients with PMI (n=225)	Patients without PMI (n=1830)		
rs6828577	rs6822035	A-A	0.3956	0.2874	1.65 (1.33 to 2.06)	$8.84 \times 10^{-6}$
rs6828577	rs6822035	G-C	0.6044	0.7126	Reference	
rs6822035	rs10518325	A-G	0.03516	0.0528	0.86 (0.43 to 1.70)	0.657
rs6822035	rs10518325	C-G	0.009083	0.02636	1.39 (0.67 to 2.90)	0.378
rs6822035	rs10518325	A-A	0.3631	0.2358	1.87 (1.46 to 2.39)	$5.54 \times 10^{-7}$
rs6822035	rs10518325	C-A	0.5927	0.685	Reference	
rs10518325	rs11098451	A-A	0.03097	0.06231	0.76 (0.48 to 1.19)	0.225
rs10518325	rs11098451	G-G	0.04425	0.07845	0.87 (0.58 to 1.31)	0.509
rs10518325	rs11098451	A-G	0.9248	0.8592	Reference	

Adjusted for clinical characteristics including extracardiac arteriopathy, recent myocardial infarction, procedure other than CABG only, year of surgery, number of diseased vessels, aortic cross-clamp time.

CABG, coronary artery bypass grafting; PMI, perioperative myocardial infarction; SNP, single nucleotide polymorphism.

promoting myocardial repair. Genetic variants in HDACs are important determinants of susceptibility to cardiovascular diseases,<sup>32</sup> suggesting functional roles for HDAC4 in modulating perioperative myonecrosis, and their potential use in predicting individual patient responsiveness to HDAC inhibition.

One of the intergenic SNPs associated with PMI (rs609418) is located near the mother against the decapentaplegic homologue 9 (*SMAD9*) gene, part of the transforming growth factor  $\beta$  (TGF- $\beta$ ) signalling pathway, which is markedly activated in the infarcted myocardium. Members of the TGF- $\beta$  superfamily transduce their signal from the membrane to the nucleus via a distinct combination of transmembrane receptors and downstream effectors—the SMAD proteins.<sup>33</sup> TGF- $\beta$  plays important and complex roles in regulating postinfarction inflammatory responses. In animal models, signalling through the SMAD transcription factors is associated with resolution of inflammation, repression of cytokine and chemokine gene synthesis, and protection against myocardial ischaemia-reperfusion injury.<sup>34</sup> Consistent with this single-locus gene association result, the bone morphogenetic protein pathway, which also transduces its signals via a SMAD9-dependent cascade, was identified as one of the top-scoring pathways in our GWAS pathway analysis ( $p=5.2\times 10^{-3}$ , see online supplementary table S7). Although no direct functional roles are currently attributed to this intergenic region, a query of the Regulome and Haploreg databases reports that rs609418 is located within active regulatory elements (GATA2 transcription factor binding site by ENCODE ChIP-seq and altering regulatory motifs in Gfi1 and Mef2 by the Position-Weight Matrix, see online supplementary figure S7).

Surprisingly, we have been unable to replicate previously reported associations between common genetic variants at the 9p21 locus and risk for PMI or mortality after CABG.<sup>8–9</sup> Many different reasons may account for this, including inadequate sample size, variation in study design, differences in allele frequencies or variability in the definition of PMI phenotype.<sup>35</sup> Indeed, our observation is consistent with other studies showing that, although genetic variants at the 9p21 locus are associated with incident coronary artery disease (CAD), they may not be associated with the actual risk of MI.<sup>36</sup> This discrepancy between convincing associations of 9p21 with a greater burden of CAD but not with MI in the presence of underlying CAD has been further confirmed by nested case-control studies<sup>37</sup> as well as meta-analyses.<sup>5 38 39</sup> Taken together, in subjects with established CAD, such as those included in our study, any lack of association of the 9p21 locus with subsequent MI could have resulted from the presence of CAD in carriers and non-carriers of the risk variants at the 9p21 locus, which seems to primarily mediate an atherosclerotic phenotype.

The strengths of our study are (1) a relatively large population of cardiac surgery patients, (2) a prospective cohort design and (3) a combination of complementary

single-marker and pathway-based genome-wide association analyses. This approach allowed us to identify genetic variants that carry only a small disease risk individually, but that jointly can contribute relatively large effects on PMI susceptibility. Furthermore, an application of results from pathway-based analysis may add structure to interpreting genomic data and allow exploration of cellular processes that functionally underpin the observed associations. Finally, by using this approach, replication of association findings at the gene and pathway level is much easier compared to replication at the individual SNP level.<sup>13</sup> Of note, most of the genes identified through pathway enrichment analysis in this study encode targets for therapeutic drugs that have already been developed. Thus, by improving risk assessment and identifying allele-specific therapeutic responses, further investigation of loci and pathways prioritised in this study could yield actionable results for enhancing perioperative cardioprotection.

Several limitations are worth mentioning. Power calculations (see online supplementary results B.6.) show that, based on the current sample size and incidence of PMI, our study can detect a genotypic relative risk approximately 2 with 80% power (assuming a variant with a 10% minor allele frequency and a realistic linkage disequilibrium between the tested marker and the causal locus  $D'=0.8$ ). Thus, although our study is the largest genetic association study of PMI conducted to date, it is powered to detect only common variants with relatively large effect sizes. Most published genetic association studies of PMI have reported larger effect sizes compared with ambulatory populations (OR range 1.79–3.97).<sup>8 10 11</sup> The possibility of rare genetic variants that drive a pronounced clinical phenotype was not explored in this study, because only variants with minor allele frequencies  $>0.05$  were assessed. Also, functional studies to further elucidate the potential biological effects of the SNPs identified were not feasible due to lack of plasma or tissue availability in the GeneMAGIC study. Finally, patients enrolled in our cohorts were predominantly Caucasian, and therefore our findings cannot be generalised to other ethnic groups.

In conclusion, we report the first GWAS in a cohort of patients at risk for MI after CABG surgery. On the basis of our integrated approach utilising primary (PMI) and secondary phenotypes (quantitative CK-MB, extreme CK-MB), single-marker analysis and pathway analysis, we identified several polymorphisms in the insulin growth factor system implicated in the regulation of extracellular matrix remodelling, as well as the ER-to-Golgi secretory pathway potentially involved in adaptive responses to ER stress. As other GWAS of PMI cohorts publish their results, we intend to collaborate on conducting a meta-analysis for this particular phenotype. While our GWAS results are intriguing, follow-up studies are needed to translate these initial findings into biological insights that could lead to predictive and therapeutic advances in perioperative care. For instance, in the

regions of confirmed associations, causal variants will only occasionally be among those directly genotyped. Moreover, GWAS detect almost exclusively the effects of common SNPs, offering limited power to capture any rare and structural variants, such as insertions, deletions, inversions and translocations. Detailed sequencing may be necessary to further characterise the genetic variations in the PMI-associated regions to enhance the identification of causal variants. Furthermore, as in most cases, the functions of identified genes and their variants, as well as the mechanisms by which they may contribute to PMI pathophysiology, are largely unknown. Currently, very few existing groups can bridge from genetics to molecular biology or cell physiology and to disease or novel therapy; we propose to examine the mechanisms by which variation in the observed genes is involved in myocardial ischaemia-reperfusion injury by examining their functional effects in the human myocardium from patients undergoing cardiac surgery, as well in our previously described preclinical rodent and swine models of cardioplegic arrest and cardiopulmonary bypass.<sup>40</sup> The use of such animal models would allow pharmacological studies targeting the identified pathways to explore the mechanism by which novel cardioprotective drugs would attenuate myocardial ischaemia-reperfusion injury, with the ultimate goal of developing personalised cardioprotective strategies.

#### Author affiliations

<sup>1</sup>Division of Cardiothoracic Anesthesiology, Duke University, Durham, North Carolina, USA

<sup>2</sup>Department of Biostatistics and Bioinformatics, Duke University, Durham, North Carolina, USA

<sup>3</sup>Duke Molecular Physiology Institute; Duke University, Durham, North Carolina, USA

<sup>4</sup>Division of Cardiology, Duke University, Durham, North Carolina, USA

<sup>5</sup>Duke Clinical Research Institute; Duke University, Durham, North Carolina, USA

<sup>6</sup>Cardiac Surgery; Duke University, Durham, North Carolina, USA

**Contributors** MDK contributed to the analysis and interpretation of data, as well as the drafting of the manuscript. Y-JL contributed to the analysis and interpretation of data and a critical revision of the manuscript. Y-JL and Y-WL contributed to the quality control and analysis of the data. JA, MFN, PKS, DJ and JPM contributed to the acquisition of data and a critical review of the manuscript. MVP contributed to the conception and design, analysis and interpretation of data, critical manuscript review and approved the final version of the submitted manuscript.

**Funding** This work was supported in part by the National Institutes of Health grants R01-HL075273 and R01-HL092071 (to MVP) and by the American Heart Association grants 0256342U and 9951185U (to JPM), and 0120492U (to MVP).

**Competing interests** None.

**Patient consent** Obtained.

**Ethics approval** The Duke University School of Medicine Institutional Review Board.

**Provenance and peer review** Not commissioned; externally peer reviewed.

**Data sharing statement** No additional data are available.

**Open Access** This is an Open Access article distributed in accordance with the Creative Commons Attribution Non Commercial (CC BY-NC 4.0) license, which permits others to distribute, remix, adapt, build upon this work non-commercially, and license their derivative works on different terms, provided

the original work is properly cited and the use is non-commercial. See: <http://creativecommons.org/licenses/by-nc/4.0/>

#### REFERENCES

- Domanski MJ, Mahaffey K, Hasselblad V, *et al.* Association of myocardial enzyme elevation and survival following coronary artery bypass graft surgery. *JAMA* 2011;305:585–91.
- Schwartz Longacre L, Kloner RA, Arai AE, *et al.* New horizons in cardioprotection: recommendations from the 2010 National Heart, Lung, and Blood Institute Workshop. *Circulation* 2011;124:1172–9.
- Samani NJ, Erdmann J, Hall AS, *et al.* Genome-wide association analysis of coronary artery disease. *N Engl J Med* 2007;357:443–53.
- McPherson R, Pertsemidis A, Kavaslar N, *et al.* A common allele on chromosome 9 associated with coronary heart disease. *Science* 2007;316:1488–91.
- Schunkert H, Gotz A, Braund P, *et al.* Repeated replication and a prospective meta-analysis of the association between chromosome 9p21.3 and coronary artery disease. *Circulation* 2008;117:1675–84.
- Kathiresan S, Voight BF, Purcell S, *et al.* Genome-wide association of early-onset myocardial infarction with single nucleotide polymorphisms and copy number variants. *Nat Genet* 2009;41:334–41.
- Pankow JS, Folsom AR, Cushman M, *et al.* Familial and genetic determinants of systemic markers of inflammation: the NHLBI family heart study. *Atherosclerosis* 2001;154:681–9.
- Liu KY, Muehlschlegel JD, Perry TE, *et al.* Common genetic variants on chromosome 9p21 predict perioperative myocardial injury after coronary artery bypass graft surgery. *J Thorac Cardiovasc Surg* 2010;139:483–8, 88 e1–2.
- Muehlschlegel JD, Liu KY, Perry TE, *et al.* Chromosome 9p21 variant predicts mortality after coronary artery bypass graft surgery. *Circulation* 2010;122(11 Suppl):S60–5.
- Collard CD, Sherman SK, Fox AA, *et al.* The MBL2 'LYQA secretor' haplotype is an independent predictor of postoperative myocardial infarction in whites undergoing coronary artery bypass graft surgery. *Circulation* 2007;116(11 Suppl):I106–12.
- Podgoreanu MV, White WD, Morris RW, *et al.* Inflammatory gene polymorphisms and risk of postoperative myocardial infarction after cardiac surgery. *Circulation* 2006;114(1 Suppl):I275–81.
- Lobato RL, White WD, Mathew JP, *et al.* Thrombomodulin gene variants are associated with increased mortality after coronary artery bypass surgery in replicated analyses. *Circulation* 2011;124(11 Suppl):S143–8.
- Luo L, Peng G, Zhu Y, *et al.* Genome-wide gene and pathway analysis. *Eur J Hum Genet* 2010;18:1045–53.
- Torkamani A, Topol EJ, Schork NJ. Pathway analysis of seven common diseases assessed by genome-wide association. *Genomics* 2008;92:265–72.
- Khoriaty R, Vasievich MP, Ginsburg D. The COPII pathway and hematologic disease. *Blood* 2012;120:31–8.
- Little J, Higgins JP, Ioannidis JP, *et al.* Strengthening the reporting of genetic association studies (STREGA): an extension of the STROBE Statement. *Hum Genet* 2009;125:131–51.
- Skol AD, Scott LJ, Abecasis GR, *et al.* Optimal designs for two-stage genome-wide association studies. *Genet Epidemiol* 2007;31:776–88.
- Alexander JH, Hafley G, Harrington RA, *et al.* Efficacy and safety of edifoligide, an E2F transcription factor decoy, for prevention of vein graft failure following coronary artery bypass graft surgery: PREVENT IV: a randomized controlled trial. *JAMA* 2005;294:2446–54.
- Thygesen K, Alpert JS, Jaffe AS, *et al.* Third universal definition of myocardial infarction. *Circulation* 2012;126:2020–35.
- Helgadottir A, Thorleifsson G, Manolescu A, *et al.* A common variant on chromosome 9p21 affects the risk of myocardial infarction. *Science* 2007;316:1491–3.
- Price AL, Patterson NJ, Plenge RM, *et al.* Principal components analysis corrects for stratification in genome-wide association studies. *Nat Genet* 2006;38:904–9.
- Fox RM, Hanlon CD, Andrew DJ. The CrebA/Creb3-like transcription factors are major and direct regulators of secretory capacity. *J Cell Biol* 2010;191:479–92.
- Ahyi AN, Quinton LJ, Jones MR, *et al.* Roles of STAT3 in protein secretion pathways during the acute-phase response. *Infect Immun* 2013;81:1644–53.
- Unlu G, Levic DS, Melville DB, *et al.* Trafficking mechanisms of extracellular matrix macromolecules: insights from vertebrate development and human diseases. *Int J Biochem Cell Biol* 2014;47:57–67.

25. Baines AC, Adams EJ, Zhang B, *et al.* Disruption of the Sec24d gene results in early embryonic lethality in the mouse. *PLoS ONE* 2013;8:e61114.
26. Kluge A, Zimmermann R, Munkel B, *et al.* Insulin-like growth factor I is involved in inflammation linked angiogenic processes after microembolisation in porcine heart. *Cardiovasc Res* 1995;29:407–15.
27. Kluge A, Zimmermann R, Munkel B, *et al.* Insulin-like growth factor II is an experimental stress inducible gene in a porcine model of brief coronary occlusions. *Cardiovasc Res* 1995;29:708–16.
28. Vogt AM, Htun P, Kluge A, *et al.* Insulin-like growth factor-II delays myocardial infarction in experimental coronary artery occlusion. *Cardiovasc Res* 1997;33:469–77.
29. Heeschen C, Dimmeler S, Hamm CW, *et al.* Pregnancy-associated plasma protein-A levels in patients with acute coronary syndromes: comparison with markers of systemic inflammation, platelet activation, and myocardial necrosis. *J Am Coll Cardiol* 2005;45:229–37.
30. Conti E, Andreotti F, Zuppi C. Pregnancy-associated plasma protein a as predictor of outcome in patients with suspected acute coronary syndromes. *Circulation* 2004;109:e211–12; author reply e11–2.
31. Granger A, Abdullah I, Huebner F, *et al.* Histone deacetylase inhibition reduces myocardial ischemia-reperfusion injury in mice. *Faseb J* 2008;22:3549–60.
32. Backs J, Olson EN. Control of cardiac growth by histone acetylation/deacetylation. *Circ Res* 2006;98:15–24.
33. Bujak M, Frangogiannis NG. The role of TGF-beta signaling in myocardial infarction and cardiac remodeling. *Cardiovasc Res* 2007;74:184–95.
34. Kempf T, Eden M, Strelau J, *et al.* The transforming growth factor-beta superfamily member growth-differentiation factor-15 protects the heart from ischemia/reperfusion injury. *Circ Res* 2006;98:351–60.
35. Lim CC, van Gaal WJ, Testa L, *et al.* With the “universal definition,” measurement of creatine kinase-myocardial band rather than troponin allows more accurate diagnosis of periprocedural necrosis and infarction after coronary intervention. *J Am Coll Cardiol* 2011;57:653–61.
36. Virani SS, Brautbar A, Lee VV, *et al.* Chromosome 9p21 single nucleotide polymorphisms are not associated with recurrent myocardial infarction in patients with established coronary artery disease. *Circ J* 2012;76:950–6.
37. Home BD, Carlquist JF, Muhlestein JB, *et al.* Association of variation in the chromosome 9p21 locus with myocardial infarction versus chronic coronary artery disease. *Circ Cardiovasc Genet* 2008;1:85–92.
38. Chan K, Patel RS, Newcombe P, *et al.* Association between the chromosome 9p21 locus and angiographic coronary artery disease burden: a collaborative meta-analysis. *J Am Coll Cardiol* 2013;61:957–70.
39. Patel RS, Asselbergs FW, Quyyumi AA, *et al.* Genetic variants at chromosome 9p21 and risk of first versus subsequent coronary heart disease events: a systematic review and meta-analysis. *J Am Coll Cardiol* 2014;63:2234–45.
40. de Lange F, Yoshitani K, Podgoreanu MV, *et al.* A novel survival model of cardioplegic arrest and cardiopulmonary bypass in rats: a methodology paper. *J Cardiothorac Surg* 2008;3:51.

## SUPPLEMENTAL MATERIAL

### **Table of Contents**

PEGASUS Investigative Team Members	Page 2
<b>Supplemental Methods</b>	Page 3
A.1. Quality control of data flow	Page 3
A.2. Controlling for population stratification	Page 4
A.3. Haplotype analysis	Page 6
A.4. GWAS pathway analysis	Page 6
<b>Supplemental Results</b>	Page 7
B.1. Patient characteristics	Page 7
B.2. Single-locus GWAS analysis	Page 8
B.3. Haplotype analysis	Page 8
B.4. Chromosome 9p21 locus analysis	Page 14
B.5. GWAS pathway analysis results	Page 15
B.6. Power calculation	Page 21
B.7. Details of the top 521 SNPs identified in stage I GWAS analyses	Page 22
<b>Supplemental References</b>	Page 25

**Perioperative Genetics and Safety Outcomes Study (PEGASUS) Investigative Team Members**

Allen AS, Davis RD, Funk B, Gaca JG, Ginsburg GS, Glower DD, Goldstein DB, Grichnik KP, Hall RL, Hauser E, Jones R, Kertai MD, Laskowitz DT, Li YJ, Lodge AJ, Mathew JP, Milano CA, Moretti EW, Newman MF, Phillips-Bute B, Podgoreanu MV, Smith MP, Smith PK, Stafford-Smith M, Swaminathan M, Welsby IJ, White WD, Willard HF

## A. SUPPLEMENTAL METHODS

### A.1. Quality control of data flow

The following quality control steps were taken to make sure that genotypes were correctly called.

- Infinium BeadStudio raw data analysis: Any sample that had a very low intensity or a very low call rate using the standard Illumina cluster ( $< 95\%$ ) was deleted. All SNPs that had a call frequency below 100% were then reclustered. Any sample that was below a 98% call rate after reclustering was deleted. Next, all SNPs that had a call frequency below 99% were deleted. Any SNPs for which  $>1\%$  of samples were not called or were ambiguously called were deleted. A total of 35 samples (13 in GeneMagic and 22 in PEGASUS cohort) were deleted during this procedure.
- Minor allele frequency (MAF) check for data handling accuracy: This step performs a basic check of the data accuracy on the data flow pipeline from the output of the Illumina genotyping facility to the analytical process. We checked the MAF report from PLINK software against the original locus report generated by the genotyping facility, and ensured that the 2 matched exactly.
- Gender specification: This step compares the observed genotypes on chromosomes X and Y to the gender specification obtained from the phenotype database. Samples with X-chromosomal heterozygosity that was inconsistent with reported gender were individually inspected against the original data source. A total of 11 samples could not be reconciled and were excluded at this step (8 in GeneMagic and 3 in PEGASUS cohort)
- Cryptic relatedness: We estimated the sharing of genetic information between cohort participants by calculating identity by descent (IBD) using PLINK software. All pairs with DNA samples showing  $\geq 0.125$  estimated proportion of alleles IBD were inspected, and one sample from each pair was excluded from further analyses. A total of 9 samples (all in PEGASUS cohort) were excluded at this step.
- Genotype missing: This step assesses whether the genotype missing is skewed toward cases or controls, which could give rise to spurious association p-values. We used PLINK software to perform this check on the top SNPs discussed in the paper.

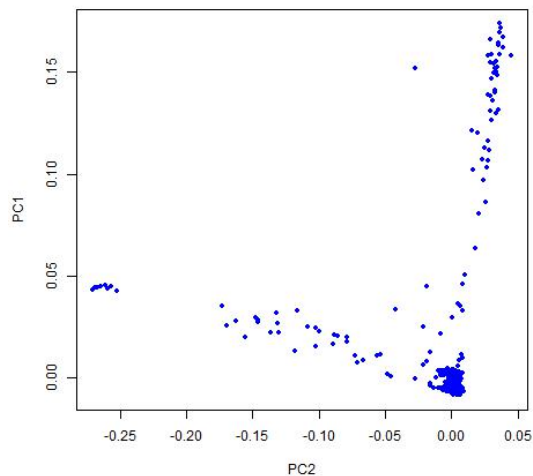
- Low MAF: We removed all SNPs with  $MAF < 0.01$  in order to control for error in the estimation of asymptotic p-values, as alleles with such a low MAF would have no chance of approaching significance based on our sample size and perioperative MI incidence.
- Hardy-Weinberg Equilibrium (HWE): We used PLINK software to identify any observed genotypes that deviated from HWE. All markers that significantly deviated from HWE ( $p < 10^{-6}$ ) were excluded.

Analyses were performed using PLINK 1.07, SAS/Genetics version 9.2, and R version 2.15.1.

## A.2. Controlling for population stratification

We used a modified EIGENSTRAT method to control for population stratification.<sup>1</sup> This method derives the principal components of the correlations among the gene variants, and corrects for those correlations in the association tests. Population structure was investigated using the EigenSoft program. All 15 principal components (PCs) were computed for both datasets. Plots between pairwise PCs, particularly PC1 vs PC2, were generated to determine whether any obvious outliers deviated from the main cluster, and hence, had to be excluded from subsequent analyses (**Supplemental Figure S1**).

**Supplemental Figure S1.** Comparison of PC1 vs PC2 reveals potential population stratification in the discovery (Gene-Magic) dataset.



In addition, we performed multivariate regression analyses using a strategy to keep all PCs up to the last PC with  $p < 0.05$  in each step, to determine the number of PCs to be used for correction in the final analysis. For instance, starting with 15 PCs in the model, if PC(i) is the last PC with  $p < 0.05$ , we included PC(1) to PC(i) in the next multivariate model, and then repeated the process until the last PC remained nominally significant. Using this iterative multivariate analysis, we found that the top 10 PCs were a reasonable set for the Gene-Magic dataset ( $p = 0.032$ ), and were subsequently re-estimated and used for stage II analysis (**Supplemental Table S1**). This final set of 10 PCs was then used as covariates to adjust for ancestry, along with clinical variables, in multivariate logistic regression analysis of perioperative MI.

**Supplemental Table S1:** Principal component analysis of the study populations

Parameter	ANALYSIS OF MAXIMUM LIKELIHOOD ESTIMATES									
	DISCOVERY DATASET					REPLICATION DATASET				
	DF	Estimate	Standard error	Wald chi-square test	P-value	DF	Estimate	Standard error	Wald chi-square test	P-value
Intercept	1	-2.635	0.127	434.325	<0.0001	1	-2.153	0.076	798.277	<0.0001
Principal component 1	1	-31.474	14.214	4.903	0.027	1	18.429	8.413	4.798	0.029
Principal component 2	1	-5.486	3.826	2.056	0.152	1	-4.009	3.338	1.443	0.230
Principal component 3	1	-7.575	3.497	4.691	0.03	1	-3.239	3.230	1.006	0.316
Principal component 4	1	-0.431	3.479	0.015	0.901	1	-1.266	3.119	0.165	0.685
Principal component 5	1	18.941	9.623	3.874	0.049	1	-1.642	4.828	0.116	0.734
Principal component 6	1	0.519	7.944	0.004	0.948	1	-15.494	7.678	4.073	0.044
Principal component 7	1	-2.231	10.001	0.049	0.824	1	12.985	6.873	3.569	0.059
Principal component 8	1	-10.793	9.043	1.424	0.233	1	2.244	4.825	0.216	0.642
Principal component 9	1	29.876	11.661	6.564	0.01	1	-8.120	5.366	2.289	0.130
Principal component 10	1	-22.775	10.593	4.623	0.032	1	7.487	4.650	2.592	0.107

DF, degrees of freedom

### **A.3. Haplotype analysis**

For the final candidate genes prioritized based on the significance of SNP association tests, we first identified the linkage disequilibrium (LD) blocks harboring the significant SNPs. Within each LD block, we performed haplotype association analysis using sliding windows of 3 markers across the region. This was conducted for the expanded dataset, by constructing multivariable logistic regression models adjusting for the same clinical covariates and PCs used for single marker analyses.

### **A.4. GWAS pathway analysis**

SNPs with a covariate-adjusted association p-value  $< 0.01$  in stage I GWAS were subjected to functional ontology enrichment analyses using tools implemented in the MetaCore software suite (GeneGO, St. Joseph, MI). Enrichment analysis begins by assigning SNPs to genes, and matching these geneIDs with geneIDs in functional ontologies in highly curated canonical pathway maps in MetaCore. The aggregation of GWAS associations for the genes in tested pathways, ie, the significance of enrichment, is computed as the p-value of a hypergeometric model.<sup>2</sup> Canonical pathways enriched in stage I and stage II analyses were further compared; and the probability of a random intersection between the set of genes in common in the 2 cohorts, and functional ontology entities was estimated as p-value of a hypergeometric distribution in MetaCore.

## B. SUPPLEMENTAL RESULTS

### B.1. Patient characteristics

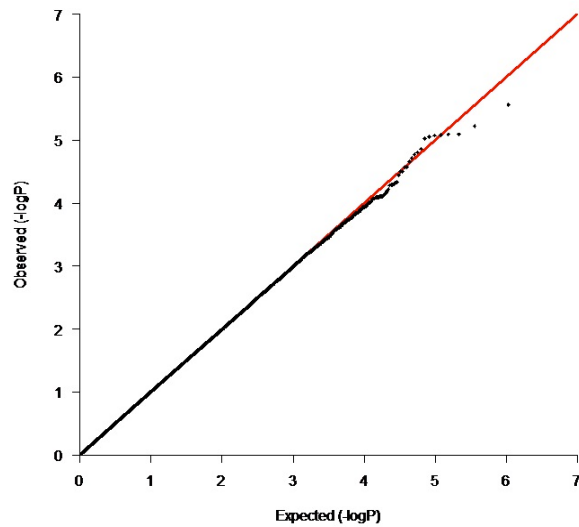
**Supplemental Table S2.** Clinical characteristics of the study populations

Characteristics	STAGE I ANALYSIS (N=1433)				STAGE II ANALYSIS (N=2055)			
	No PMI, (n=1321)	PMI (n=112)	OR (95%CI)	P-value*	No PMI (n=1830)	PMI (n=225)	OR (95%CI)	P-value*
Extracardiac arteriopathy	251 (19.0)	20 (17.9)	0.93 (0.56-1.53)	0.77	754 (41.2)	128 (56.9)	1.88 (1.42-2.49)	<0.0001
Recent myocardial infarction	256 (19.4)	23 (20.5)	1.08 (0.67-1.74)	0.77	393 (21.5)	39 (17.3)	0.77 (0.53-1.10)	0.15
Procedure other than CABG only	126 (9.5)	23 (20.5)	2.45 (1.50-4.02)	0.0004	153 (8.4)	51 (22.7)	3.21 (2.26-4.58)	<0.0001
Year of surgery by year								
1997					26 (1.4)	3 (1.3)	1.0	
1998					70 (3.8)	8 (3.6)	0.99 (0.24-4.02)	0.98
1999					87 (4.8)	3 (1.3)	0.30 (0.06-1.57)	0.15
2000					77 (4.2)	14 (6.2)	1.58 (0.42-5.92)	0.50
2001					49 (2.7)	12 (5.3)	2.12 (0.55-8.20)	0.28
2002	146 (11.1)	9 (8.0)	1.0		188 (10.3)	20 (8.9)	0.92 (0.26-3.32)	0.90
2003	1175 (88.9)	103 (92.0)	1.42 (0.70-2.87)	0.33	1189 (65.0)	109 (48.4)	0.80 (0.24-2.67)	0.71
2004					32 (1.8)	8 (3.6)	2.17 (0.52-9.0)	0.29
2005					80 (4.4)	36 (16.0)	3.90 (1.11-13.72)	0.03
2006					32 (1.8)	12 (5.3)	3.25 (0.83-12.75)	0.09
Number of diseased vessels								
0	67 (5.1)	6 (5.3)	1.0		69 (3.8)	6 (2.7)	1.0	
1	259 (19.6)	29 (25.9)	1.25 (0.50-3.14)	0.63	276 (15.0)	32 (14.2)	1.33 (0.54-3.32)	0.54
2	519 (39.3)	43 (38.4)	0.93 (0.38-2.26)	0.86	595 (32.5)	52 (23.1)	1.01 (0.42-2.43)	0.99
3	476 (36.0)	34 (30.4)	0.80 (0.32-1.97)	0.62	885 (48.4)	130 (57.8)	1.69 (0.72-3.97)	0.22
4					5 (0.3)	5 (2.2)	11.5 (2.58-51.24)	0.0014
Aortic cross clamp time, min	51.2±36.8	71.9±32.4	1.015 (1.01-1.02)	<0.0001	55.0±35.2	80.5±36.7	1.019 (1.015-1.023)	<0.0001

Descriptive statistics of clinical variables are presented as count (percent frequency) for categorical variables and mean  $\pm$  SD for continuous variables. PMI, postoperative myocardial infarction; CABG, coronary artery bypass surgery; extracardiac arteriopathy, defined as any one or more of the following: claudication, carotid occlusion or  $> 50\%$  stenosis, and/or previous or planned intervention on the abdominal aorta, limb arteries or carotids; OR (95%CI), univariate odds ratio (95% confidence interval). \*Comparisons made using the *t*-test or Wald chi-square test, as appropriate. Clinical variables were included in the final multivariate logistic regression analysis if significant ( $p < 0.05$ ) in univariate analyses.

## B.2. Single-locus GWAS analysis - population structure adjustment

**Supplemental Figure S2.** Quantile - Quantile (Q-Q) plot representation of the GWAS association results in the discovery dataset

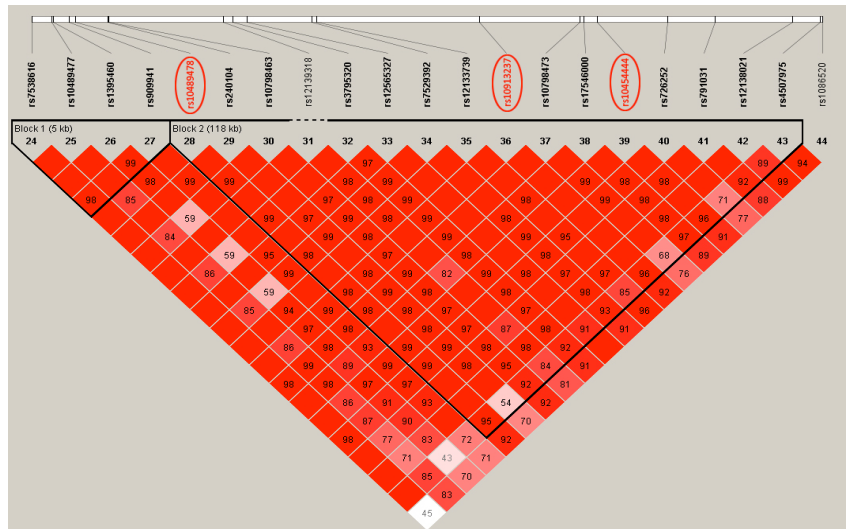


Distribution of expected (under the null hypothesis) vs observed p-values for single nucleotide polymorphisms that are associated with perioperative myocardial infarction, based on a whole genome-wide analysis. The red diagonal line represents the line obtained if the observed distribution did not deviate from the expected distribution. All p-values were corrected for the inflation factor ( $\lambda = 1.0073$ ).

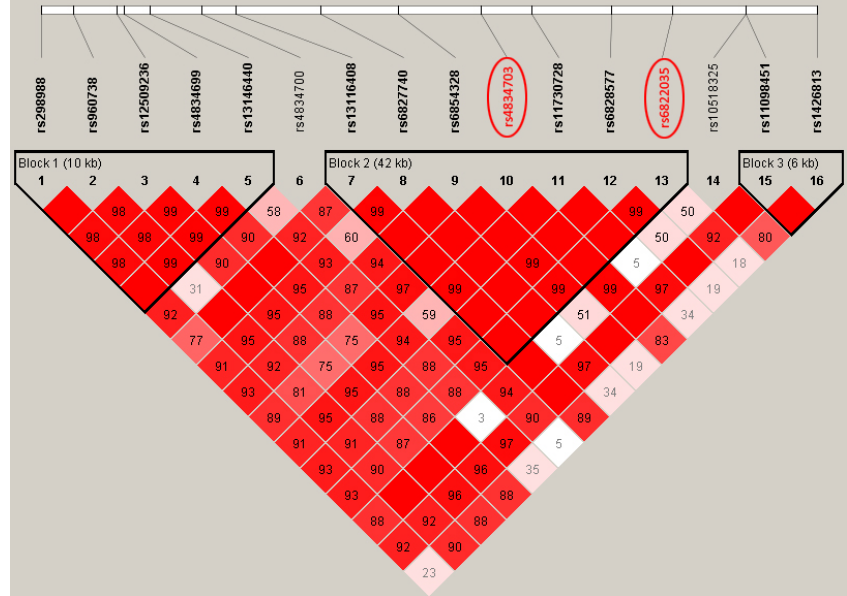
## B.3. Haplotype analysis of genes harboring top scoring SNPs

**Supplemental Figure S3.** Linkage disequilibrium (LD) structures of [A] *PAPPA2* (1q23-q25 chromosome region), [B] *SEC24D* (4q26 chromosome region), and [C] *HDAC4* (2q37.3 chromosome region), and displayed as pairwise correlation plots using HapMap database (CEU European ancestry) (Haploview). Regions of LD are shaded in bright red (strong LD) and lighter for moderate or weak LD. The physical location of the individual SNPs associated with perioperative myocardial infarction in 2-stage analyses is circled in red. True haplotype blocks in the population are marked with black lines in the correlation plot.

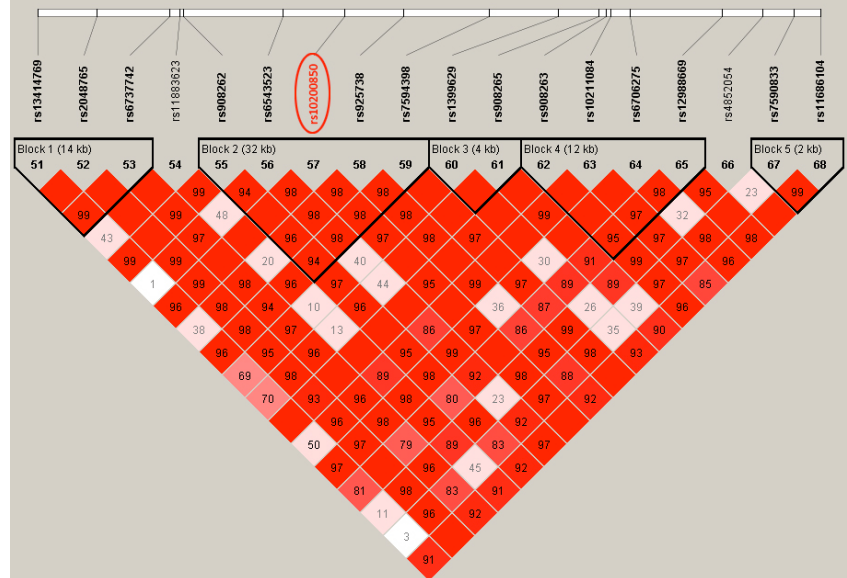
**A. *PAPPA2* gene**



**B. *SEC24D* gene**



**C. *HDAC4* gene**



**Supplemental Table S3.** Results of the haplotype analyses for *PAPPA2* and *HDAC4*

CHR	GENESYMBOL	BPI	BP2	SNP1	SNP2	HAPLOTYPE	F	OR	STAT	P
1	PAPPA2	176562608	176562796	RS10489477	RS1395460	AA	0.166	0.464	19.5	1.01E-05
1	PAPPA2	176562608	176562796	RS10489477	RS1395460	GG	0.655	1.43	9.56	0.00199
1	PAPPA2	176562608	176562796	RS10489477	RS1395460	GA	0.179	1.08	0.292	0.589
1	PAPPA2	176562796	176565307	RS1395460	RS909941	AG	0.344	0.698	9.56	0.00198
1	PAPPA2	176562796	176565307	RS1395460	RS909941	GA	0.576	1.29	5.58	0.0182
1	PAPPA2	176562796	176565307	RS1395460	RS909941	GG	0.0786	1.22	1.16	0.282
1	PAPPA2	176565307	176566350	RS909941	RS10489478	GA	0.175	0.474	20.8	4.98E-06
1	PAPPA2	176565307	176566350	RS909941	RS10489478	AG	0.578	1.29	5.55	0.0184
1	PAPPA2	176565307	176566350	RS909941	RS10489478	GG	0.248	1.19	2.17	0.141
1	PAPPA2	176566350	176571431	RS10489478	RS240104	AG	0.175	0.474	20.8	4.98E-06
1	PAPPA2	176566350	176571431	RS10489478	RS240104	GG	0.589	1.25	4.47	0.0345
1	PAPPA2	176566350	176571431	RS10489478	RS240104	GA	0.237	1.23	3.16	0.0754
1	PAPPA2	176571431	176571578	RS240104	RS10798463	GG	0.241	0.631	12.2	0.000477
1	PAPPA2	176571431	176571578	RS240104	RS10798463	AA	0.237	1.23	3.16	0.0754
1	PAPPA2	176571431	176571578	RS240104	RS10798463	GA	0.522	1.17	2.38	0.123
1	PAPPA2	176571578	176589732	RS10798463	RS12139318	GC	0.193	0.515	18.8	1.45E-05
1	PAPPA2	176571578	176589732	RS10798463	RS12139318	AC	0.759	1.58	12.2	0.000477
1	PAPPA2	176571578	176589732	RS10798463	RS12139318	GA	0.0485	1.28	1.24	0.266
1	PAPPA2	176589732	176591291	RS12139318	RS3795320	CC	0.197	0.5	20.3	6.47E-06
1	PAPPA2	176589732	176591291	RS12139318	RS3795320	CA	0.755	1.62	13.4	0.000248
1	PAPPA2	176589732	176591291	RS12139318	RS3795320	AC	0.0485	1.28	1.24	0.266
1	PAPPA2	176591291	176593524	RS3795320	RS12565327	CG	0.245	0.616	13.4	0.000256
1	PAPPA2	176591291	176593524	RS3795320	RS12565327	AG	0.675	1.49	11.4	0.00075
1	PAPPA2	176591291	176593524	RS3795320	RS12565327	AA	0.0795	1.02	0.0109	0.917
1	PAPPA2	176593524	176603840	RS12565327	RS7529392	GA	0.244	0.618	13.2	0.000274
1	PAPPA2	176593524	176603840	RS12565327	RS7529392	GG	0.676	1.49	11.3	0.000796
1	PAPPA2	176593524	176603840	RS12565327	RS7529392	AG	0.0801	1.02	0.00645	0.936

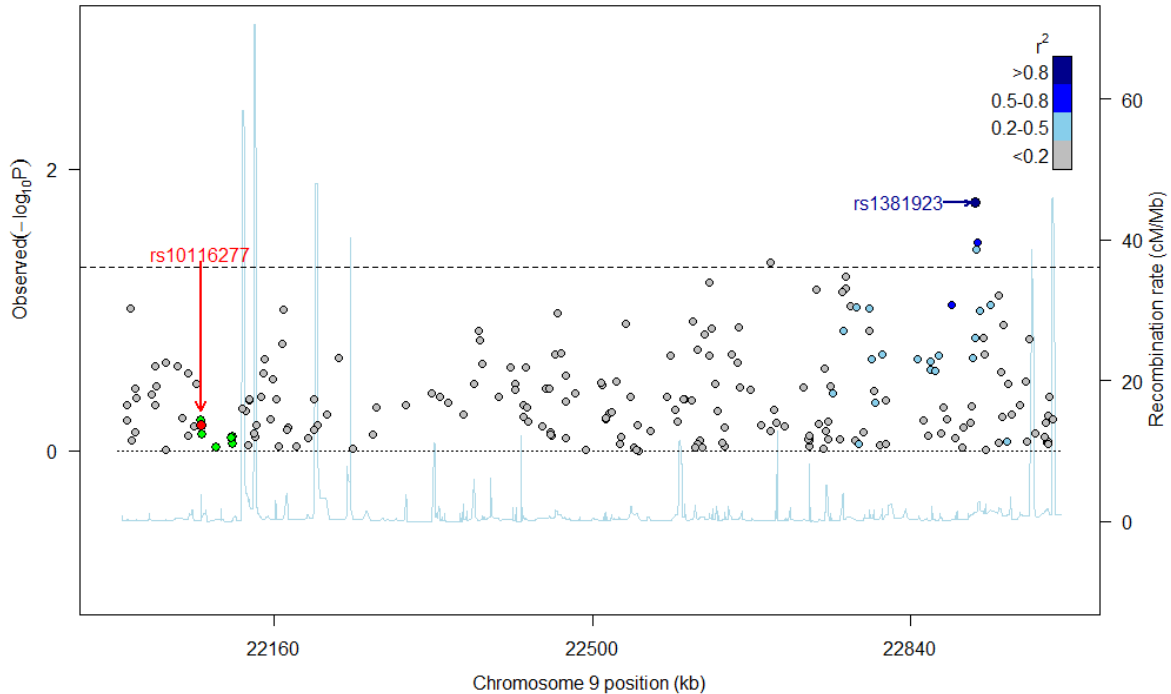
1	PAPPA2	176603840	176604564	RS7529392	RS12133739	AA	0.177	0.46	22.2	2.52E-06
1	PAPPA2	176603840	176604564	RS7529392	RS12133739	GA	0.756	1.62	13.3	0.000264
1	PAPPA2	176603840	176604564	RS7529392	RS12133739	AG	0.0675	1.23	1.13	0.288
1	<b>PAPPA2</b>	<b>176604564</b>	<b>176630416</b>	<b>RS12133739</b>	<b>RS10913237</b>	<b>AA</b>	<b>0.176</b>	<b>0.46</b>	<b>22.1</b>	<b>2.56E-06</b>
1	PAPPA2	176604564	176630416	RS12133739	RS10913237	AG	0.756	1.62	13.3	0.000269
1	PAPPA2	176604564	176630416	RS12133739	RS10913237	GG	0.0674	1.23	1.13	0.288
1	<b>PAPPA2</b>	<b>176630416</b>	<b>176646383</b>	<b>RS10913237</b>	<b>RS10798473</b>	<b>AG</b>	<b>0.176</b>	<b>0.461</b>	<b>22.1</b>	<b>2.65E-06</b>
1	PAPPA2	176630416	176646383	RS10913237	RS10798473	GA	0.489	1.29	5.98	0.0145
1	PAPPA2	176630416	176646383	RS10913237	RS10798473	GG	0.336	1.16	1.85	0.174
1	PAPPA2	176646383	176647000	RS10798473	RS17546000	GA	0.351	0.665	12.2	0.000484
1	PAPPA2	176646383	176647000	RS10798473	RS17546000	AA	0.489	1.29	5.98	0.0145
1	PAPPA2	176646383	176647000	RS10798473	RS17546000	GG	0.161	1.17	1.39	0.239
1	<b>PAPPA2</b>	<b>176647000</b>	<b>176649181</b>	<b>RS17546000</b>	<b>RS10454444</b>	<b>AG</b>	<b>0.176</b>	<b>0.461</b>	<b>22.1</b>	<b>2.60E-06</b>
1	PAPPA2	176647000	176649181	RS17546000	RS10454444	AA	0.663	1.42	9.13	0.00252
1	PAPPA2	176647000	176649181	RS17546000	RS10454444	GA	0.161	1.17	1.39	0.239
1	<b>PAPPA2</b>	<b>176649181</b>	<b>176660247</b>	<b>RS10454444</b>	<b>RS726252</b>	<b>GG</b>	<b>0.176</b>	<b>0.461</b>	<b>22.1</b>	<b>2.59E-06</b>
1	PAPPA2	176649181	176660247	RS10454444	RS726252	AA	0.591	1.28	5.11	0.0238
1	PAPPA2	176649181	176660247	RS10454444	RS726252	AG	0.232	1.23	3.09	0.0787
1	PAPPA2	176660247	176667810	RS726252	RS791031	GA	0.245	0.625	12.7	0.000371
1	PAPPA2	176660247	176667810	RS726252	RS791031	AA	0.591	1.28	5.11	0.0238
1	PAPPA2	176660247	176667810	RS726252	RS791031	GC	0.164	1.18	1.44	0.231
1	PAPPA2	176667810	176680137	RS791031	RS12138021	AA	0.769	0.832	2.43	0.119
1	PAPPA2	176667810	176680137	RS791031	RS12138021	CA	0.164	1.18	1.42	0.234
1	PAPPA2	176667810	176680137	RS791031	RS12138021	AG	0.0665	1.2	0.831	0.362
1	PAPPA2	176680137	176684432	RS12138021	RS4507975	AG	0.227	0.721	5.97	0.0146
1	PAPPA2	176680137	176684432	RS12138021	RS4507975	AA	0.706	1.23	3.05	0.0806
1	PAPPA2	176680137	176684432	RS12138021	RS4507975	GG	0.0615	1.17	0.537	0.464
2	HDAC4	240201797	240208154	RS13414769	RS2048765	GG	0.061	2.18	18.4	1.79E-05
2	HDAC4	240201797	240208154	RS13414769	RS2048765	AA	0.663	0.804	3.83	0.0503
2	HDAC4	240201797	240208154	RS13414769	RS2048765	GA	0.276	0.962	0.102	0.749
2	HDAC4	240208154	240216021	RS2048765	RS6737742	GG	0.061	2.19	18.6	1.58E-05

2	HDAC4	240208154	240216021	RS2048765	RS6737742	AG	0.718	0.773	5.06	0.0244
2	HDAC4	240208154	240216021	RS2048765	RS6737742	AA	0.221	0.986	0.012	0.913
2	HDAC4	240216021	240217116	RS6737742	RS11883623	AG	0.221	0.986	0.0128	0.91
2	HDAC4	240216021	240217116	RS6737742	RS11883623	GG	0.185	1.01	0.00304	0.956
2	HDAC4	240216021	240217116	RS6737742	RS11883623	GA	0.594	1.01	0.00252	0.96
2	HDAC4	240217116	240217522	RS11883623	RS908262	GC	0.182	1.01	0.00393	0.95
2	HDAC4	240217116	240217522	RS11883623	RS908262	AC	0.594	0.995	0.0024	0.961
2	HDAC4	240217116	240217522	RS11883623	RS908262	GA	0.224	1	0.00029	0.986
2	HDAC4	240217522	240228263	RS908262	RS6543523	CG	0.266	1.32	5.92	0.015
2	HDAC4	240217522	240228263	RS908262	RS6543523	CA	0.51	0.8	4.6	0.032
2	HDAC4	240217522	240228263	RS908262	RS6543523	AA	0.221	0.978	0.0301	0.862
2	<b>HDAC4</b>	<b>240228263</b>	<b>240234901</b>	<b>RS6543523</b>	<b>RS10200850</b>	<b>GA</b>	<b>0.0614</b>	<b>2.21</b>	<b>19.6</b>	<b>9.58E-06</b>
2	HDAC4	240228263	240234901	RS6543523	RS10200850	AG	0.73	0.75	6.47	0.011
2	HDAC4	240228263	240234901	RS6543523	RS10200850	GG	0.208	1.02	0.0282	0.867
2	HDAC4	240234901	240241255	RS10200850	RS925738	AG	0.0615	2.14	17.7	0.000026
2	HDAC4	240234901	240241255	RS10200850	RS925738	GA	0.414	0.812	3.61	0.0575
2	HDAC4	240241255	240250456	RS925738	RS7594398	GA	0.524	0.968	0.0946	0.758
2	HDAC4	240241255	240250456	RS925738	RS7594398	AG	0.0645	2.13	17.9	2.32E-05
2	HDAC4	240241255	240250456	RS925738	RS7594398	GG	0.415	0.819	3.31	0.0689
2	HDAC4	240241255	240250456	RS925738	RS7594398	GG	0.52	0.965	0.112	0.737
2	HDAC4	240250456	240257958	RS7594398	RS1399629	AA	0.0649	2.12	17.8	2.43E-05
2	HDAC4	240250456	240257958	RS7594398	RS1399629	GA	0.423	0.84	2.58	0.108
2	HDAC4	240250456	240257958	RS7594398	RS1399629	GG	0.512	0.945	0.286	0.593
2	HDAC4	240257958	240262287	RS1399629	RS908265	GG	0.13	0.905	0.388	0.533
2	HDAC4	240257958	240262287	RS1399629	RS908265	AG	0.488	1.06	0.301	0.583
2	HDAC4	240257958	240262287	RS1399629	RS908265	GA	0.382	0.986	0.0174	0.895
2	HDAC4	240262287	240263103	RS908265	RS908263	GA	0.0721	0.827	0.819	0.365
2	HDAC4	240262287	240263103	RS908265	RS908263	GG	0.546	1.07	0.387	0.534
2	HDAC4	240262287	240263103	RS908265	RS908263	AG	0.382	0.986	0.0174	0.895
2	HDAC4	240263103	240263584	RS908263	RS10211084	AG	0.0721	0.827	0.823	0.364
2	HDAC4	240263103	240263584	RS908263	RS10211084	GG	0.723	1.09	0.482	0.487

2	HDAC4	240263103	240263584	RS908263	RS10211084	GA	0.205	0.978	0.0302	0.862
2	HDAC4	240263584	240265617	RS10211084	RS6706275	GA	0.31	0.747	6.34	0.0118
2	HDAC4	240263584	240265617	RS10211084	RS6706275	GG	0.485	1.29	6.18	0.0129
2	HDAC4	240263584	240265617	RS10211084	RS6706275	AG	0.205	0.978	0.0302	0.862
2	HDAC4	240265617	240275570	RS6706275	RS12988669	AA	0.309	0.748	6.28	0.0122
2	HDAC4	240265617	240275570	RS6706275	RS12988669	GA	0.52	1.27	5.11	0.0238
2	HDAC4	240265617	240275570	RS6706275	RS12988669	GG	0.17	1.02	0.0248	0.875

#### B.4. Chromosome 9p21 locus and perioperative MI

**Supplemental Figure S4.** Single nucleotide polymorphisms at 9p21 locus previously associated with incident myocardial infarction<sup>3</sup> and mortality<sup>4</sup> after CABG.

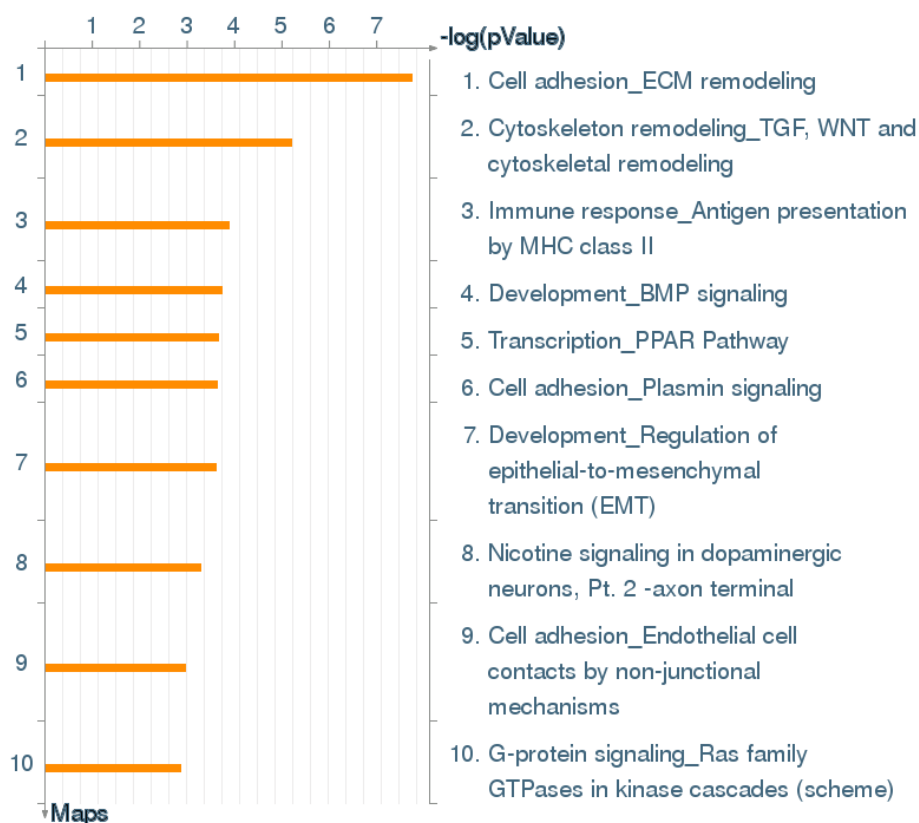


The dashed horizontal line indicates the nominal significance threshold,  $p = 0.05$ . The green dots represent single nucleotide polymorphisms (base pair) at the 9p21 locus previously identified as predictors of perioperative MI: rs1547705 (22082375, intron); rs1333040 (22083404, intron); rs4977574 (22098574, intron); rs944797 (22115286, intron); rs2383207 (22115959, intron); rs1537375 (22116071, intron). The red dot represents rs10116277 (22081397) variant, which was previously associated with myocardial infarction in both non-surgical and cardiac surgical cohorts. The dark blue point rs1381923 (22909438, unknown function) is the most significant variant in this plotted region. All p-values are the results of multivariate risk factor-adjusted analyses.

### B.5. GWAS pathway analysis results

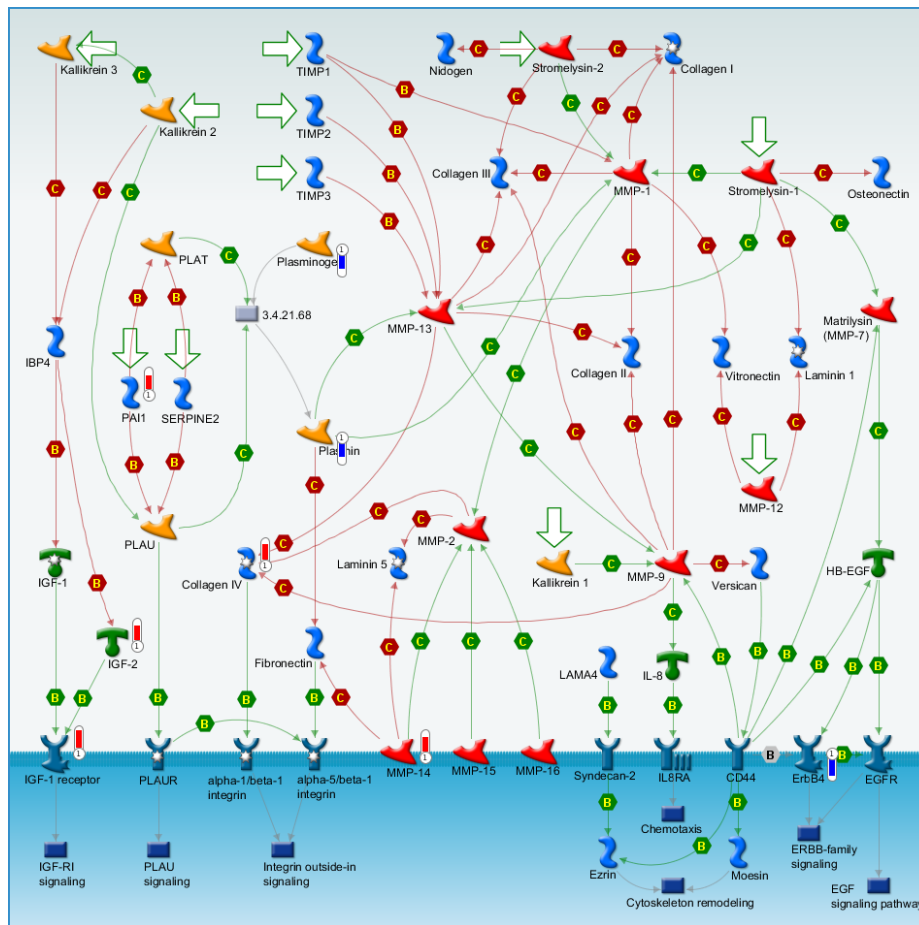
Of the 534,350 SNPs included in analysis, 250,740 were recognized, and 66,893 were mapped to 19,163 genes within MetaCore. Stage I cohort analysis in MetaCore identified several canonical pathways after functional enrichment analysis with SNPs that passed the p-value and odds-ratio filters ( $p < 0.01$ ,  $0.9 < OR < 1.1$ ).

**Supplemental Figure S5.** GenGo Canonical Pathway Maps histograms after enrichment analysis with SNPs that passed the threshold and p-value filter in GWAS stage I analyses.



The top 10 canonical maps for enriched SNPs are shown as histogram plots. Results are tabulated/sorted in the histogram based on calculated  $-\log(p\text{-values})$  of hypergeometric distribution statistics.

**Supplemental Figure S6.** The top scoring pathway map based on the enrichment distribution in GWAS stage I analysis – *Cell adhesion: extracellular matrix remodeling.*



Top-scoring SNPs based on GWAS stage I results are linked to genes and visualized on the maps as thermometer-like symbols. Up-ward thermometers are red and indicate an odds ratio  $>1$  for association with perioperative MI, and down-ward (blue) ones indicate an odds ratio for association  $<1$ . Letters “B”, and “C” indicate physical interactions, B, binding; and C, cleavage. Arrows with hexagons indicate positive (green), negative (red), and unspecified (gray) effects. Arrows without hexagons indicate technical link (gray). For further information on pathway elements please see: [http://pathwaymaps.com/pdf/MC\\_legend.pdf](http://pathwaymaps.com/pdf/MC_legend.pdf)

Top-scoring pathways in stage I analyses were compared with enriched pathways in the stage II cohort. The probability of a random intersection between a set of genes common to both cohorts with functional ontology entities was estimated as p-value of hypergeometric distribution using the Compare Experiments Workflow in MetaCore. The top 4 scored canonical pathway maps (lowest p-values), based on the enrichment distribution, are presented below.

1. Immune response NFAT signaling and leukocyte interaction ( $p = 7.2 \cdot 10^{-4}$ ). Nuclear factors of activated T-cells (NFATs) is a family of calcium-dependent transcription factors with pivotal roles in regulating immune responses, which include interactions between antigen-presenting cells and other leukocytes, and expression of a variety of cytokines by coupling changes in intracellular calcium concentration to gene expression. Variants in CD247, calcium channels, MHC class II, and NFAT that map to this pathway, and their association with perioperative MI is presented below in **Supplemental Table S4**.

SNPId	Gene Symbol	Gene Name	OR	p-value
rs2982480;rs2984800;rs2995054	CD247	CD247 molecule	2.16	0.00311
rs42051;rs7804449;rs1544462;rs1156325;rs2237526;rs2018982	CACNA2D1	calcium channel, voltage-dependent, alpha 2/delta subunit 1	0.71	0.00368
rs1779244;rs2068357	CACNB2	calcium channel, voltage-dependent, beta 2 subunit	0.50	0.00162
rs3117016;rs9380342	HLA-DPB2	major histocompatibility complex, class II, DP beta 2 (pseudogene)	2.45	0.00795
rs3129882	HLA-DRA	major histocompatibility complex, class II, DR alpha	1.49	0.00580
rs1562724;rs1017860;rs8090864	NFATC1	nuclear factor of activated T-cells, cytoplasmic, calcineurin-dependent 1	1.45	0.00362

2. Cell adhesion and extracellular matrix (ECM) remodeling ( $p = 1.1 \cdot 10^{-3}$ ). An important pathway involved in responses to myocardial injury, is comprised of matrix metalloproteinases (MMPs), their endogenous tissue inhibitors (TIMPs), and various collagens. Furthermore, the plasminogen-plasmin system and its regulators (PAI-1) are implicated in proteolytic degradation of ECM. Finally, 2 categories of growth factors are part of this canonical pathway – insulin-like growth factors 1 and 2 (IGF-1 and IGF-2), and heparin-binding EGF-like growth factor (HB-EGF) – and all are involved in regulating cell growth, proliferation, and survival. IGF-1 and IGF-2 function by activating the IGF-1 receptor, but their

bioavailability is regulated by a family of insulin-like growth factor binding proteins (IGFBP4)., HB-EGF activates the epidermal growth factor receptor (EGFR) and v-erb-a erythroblastic leukemia viral oncogene homolog 4 (ErbB4), leading to cell proliferation, cell survival, and tissue remodeling (**Supplemental Table S5**).

SNPId	Gene Symbol	Gene Name	OR	P-value
rs953386;rs2391823	COL4A1	collagen, type IV, alpha 1	1.76	0.00162
rs884904;rs845552	EGFR	epidermal growth factor receptor	1.67	0.00238
rs9288433;rs3817429;rs2371276;rs1473636;rs7425448;rs10932384;rs6740117;rs12053361;rs17803152;rs7594456;rs4672615;rs1851169;rs6747637	ERBB4	v-erb-a erythroblastic leukemia viral oncogene homolog 4 (avian)	0.53	0.00613
rs2033178	IGF1	insulin-like growth factor 1 (somatomedin C)	0.50	0.00901
rs8038056;rs8028620;rs2139924;rs3784604	IGF1R	insulin-like growth factor 1 receptor	1.90	0.00383
rs734351	IGF2	insulin-like growth factor 2 (somatomedin A)	1.57	0.00159
rs12454479;rs8086477;rs12454564	LAMA3	laminin, alpha 3	2.01	0.00165
rs762052	MMP14	matrix metalloproteinase 14 (membrane-inserted)	1.60	0.00863
rs1050813	SERPINE1	serpin peptidase inhibitor, clade E (nexin, plasminogen activator inhibitor type 1), member 1	1.38	0.00874
rs783147	PLG	plasminogen	0.68	0.00979

3. Regulation of lipid metabolism RXR-dependent regulation of lipid metabolism via PPAR, RAR, and VDR ( $p = 5.1 \times 10^{-3}$ ; **Supplemental Table S6**).

SNPId	Gene Symbol	Gene Name	OR	P-value
rs12364396	CPT1A	carnitine palmitoyltransferase 1A	1.779	0.006433
rs1286767;rs2164360;rs2033447	RARB	retinoic acid receptor, beta	1.647	0.005116

4. BMP (bone morphogenic protein) signaling pathway ( $p = 5.2 \times 10^{-3}$ ). BMPs are members of the TGF- $\beta$  superfamily, with important roles in embryonic development including cardiomyogenesis and apoptosis. BMPs transduce their signals via 2 pathways: SMAD-dependent (including SMAD9[8]), and SMAD-

independent cascade. BMP activity can be regulated by intracellular inhibitory SMADs (like SMAD6) or extracellularly by secreted antagonists (like gremlin). Variants in SMAD9 and SMAD6 were associated with an increased incidence of perioperative MI (**Supplemental Table S7**).

SNPId	Gene Symbol	Gene Name	OR	p-value
rs11858577	SMAD6	SMAD, mothers against DPP homolog 6	2.30	0.0002506
rs7998663	SMAD9	Mothers against decapentaplegic, drosophila, homolog of, 9	2.47	0.000167
rs884940	SKI	ski oncoprotein	0.61	0.0006749

In summary, functional analysis of genome-wide association data using biological ontologies allowed us to supplement our single marker analysis results by identifying a number of additional candidates for further investigation as biomarkers for perioperative MI. It also highlighted the potential mechanistic importance of several signaling pathways that have not previously been implicated in the complex and multifactorial pathogenesis of perioperative ischemia-reperfusion injury.

**Supplemental Figure S7** summarizes RegulomeDB ([regulome.stanford.edu](http://regulome.stanford.edu)) and HaploReg v2 (<http://www.broadinstitute.org/mammals/haploreg/haploreg.php>) database results for rs609408 (intergenic variant, located 1.5kb 3' of SMAD9).

#### A. RegulomeDB supporting data for rs609418

Protein Binding						Filter: <input type="text"/>
Method	Location	Bound Protein	? Cell Type	Additional Info	Reference	
ChIP-seq	chr13:37417308..37417652	GATA2	SH-SY5Y		<a href="#">ENCODE</a>	

Motifs						Filter: <input type="text"/>
Method	Location	Motif	? Cell Type	PWM	Reference	
PWM	chr13:37417418..37417435	Elf3			<a href="#">19443739</a>	

## B. HaploReg v2 summary for rs609418 and variants with $r^2 \geq 0.8$

Query SNP: **rs609418** and variants with  $r^2 \geq 0.8$

chr	pos (hg19)	LD (r)	LD (D)	variant	Ref	Alt	AFR freq	AMR freq	ASN freq	EUR freq	SiPhy cons	Promoter histone marks	Enhancer histone marks	DNase	Proteins bound	eQTL tissues	Motifs changed	GENCODE genes	dbSNP func annot	
13	37396093	0.98	-0.99	rs1980881	G	A	0.34	0.74	0.55	0.74			Huvec				5 altered motifs	RFXAP	intronic	
13	37396218	0.98	-0.99	rs1980880	A	G	0.34	0.74	0.55	0.74			Huvec, GM12878				6 altered motifs	RFXAP	intronic	
13	37400621	0.9	-0.99	rs7983276	T	A	0.33	0.76	0.55	0.76							Mef2,TATA	RFXAP	intronic	
13	37401286	0.9	-0.99	rs7984398	T	C	0.33	0.76	0.55	0.76							Foxp1,Pou2f2,TATA	RFXAP	intronic	
13	37407492	0.89	1	rs1571320	C	G	0.45	0.23	0.33	0.24			Ishikawa,HRCEpC,RPTEC				AP-1	4.3kb 3' of RFXAP		
13	37407870	0.9	1	rs4943419	C	T	0.45	0.23	0.33	0.24							TEF	4.6kb 3' of RFXAP		
13	37408545	0.9	1	rs8563501	A	G	0.45	0.23	0.33	0.24			FibroP,HMVEC-LBI,NH-A				HDAC2,Tgfi1	5.3kb 3' of RFXAP		
13	37408734	1	-1	rs9315450	T	C	0.35	0.74	0.55	0.74			4 cell types				Smad	5.5kb 3' of RFXAP		
13	37409508	0.9	1	rs9566166	G	A	0.45	0.23	0.33	0.24			Th2				Mef2,SIX5	6.3kb 3' of RFXAP		
13	37410696	1	-1	rs9315451	A	C	0.35	0.74	0.55	0.74							HDAC2	7.5kb 3' of RFXAP		
13	37410794	0.9	1	rs4943421	C	G	0.46	0.23	0.34	0.24							Zic	7.6kb 3' of RFXAP		
13	37411589	0.9	1	rs11838533	A	G	0.40	0.23	0.33	0.24			Th1				Pax-4	7.4kb 3' of SMAD9		
13	37412644	0.9	1	rs4943423	C	T	0.51	0.24	0.33	0.24							GATA	6.3kb 3' of SMAD9		
13	37413544	0.9	1	rs7982338	A	C	0.47	0.23	0.33	0.24			BE2_C,HIPEpC	SRF			CTCF,NF-1,p53	5.4kb 3' of SMAD9		
13	37413557	0.9	1	rs7981675	C	T	0.47	0.23	0.33	0.24			BE2_C,HIPEpC	SRF			4 altered motifs		4.2kb 3' of SMAD9	
13	37414795	0.9	1	rs4943426	T	C	0.46	0.23	0.34	0.24			H1				7 altered motifs		2.7kb 3' of SMAD9	
13	37416234	0.88	1	rs9635072	G	A	0.39	0.23	0.34	0.23									1.9kb 3' of SMAD9	
13	37417048	1	-1	rs7325187	G	T	0.34	0.74	0.54	0.74									6 altered motifs	1.8kb 3' of SMAD9
13	37417206	0.9	1	rs9576121	T	C	0.46	0.23	0.34	0.24									6 altered motifs	1.5kb 3' of SMAD9
13	37417427	1	1	rs609418	A	C	0.67	0.26	0.46	0.26						GATA2		Gfi1,Mef2	1.1kb 3' of SMAD9	
13	37417894	0.89	1	rs9634749	C	A	0.46	0.23	0.34	0.24								ATF3,ATF6	1.1kb 3' of SMAD9	
13	37418491	0.99	1	rs35652793	TA	T	0.67	0.26	0.46	0.26								8 altered motifs	476bp 3' of SMAD9	
13	37419042	0.83	0.98	rs60270973	AGTT	A	0.46	0.22	0.34	0.23								HEY1,Sox	SMAD9	
13	37420348	0.98	1	rs642866	A	G	0.66	0.26	0.46	0.25								12 altered motifs	SMAD9	3'-UTR
13	37423032	0.87	1	rs4943431	G	A	0.42	0.23	0.34	0.23			Huvec					4 altered motifs	SMAD9	intronic
13	37431353	0.97	1	rs10629368	A	ACT	0.80	0.28	0.51	0.25								14 altered motifs	SMAD9	intronic
13	37434744	0.95	0.99	rs636514	G	A	0.78	0.28	0.51	0.25								CACD,NRSF	SMAD9	intronic

and detailed view for rs609418

### Sequence facts

chr	pos (hg19)	Reference	Alternate	1000 Genomes Phase 1 Frequencies				Sequence constraint		dbSNP functional annotation
				AFR	AMR	ASN	EUR	by GERP	by SiPhy	
chr13	37417427	A	C	0.67	0.26	0.46	0.26	No	No	none

### Closest annotated gene

Source	Distance	Direction	ID/Link	Common name	Description
GENCODE	3'	1540	<a href="#">ENSG00000120693.9</a>	SMAD9	SMAD family member 9 [Source:HGNC Symbol;Acc:6774]
RefSeq	3'	1539	<a href="#">NM_001127217</a>	SMAD9	SMAD family member 9 [Source:HGNC Symbol;Acc:6774]

### Proteins bound by ChIP (ENCODE)

Cell ID	Protein
SH-SY5Y	GATA2

### Regulatory motifs altered

PWM	Strand	Ref	Alt	Match on:
Gfi1_2	+	10.5	11.2	Ref: TGCTATGCAGCTGGATAACTATTTCCAAAATAAATCACAAGCAGCTTTTCTGATCCCT Alt: TGCTATGCAGCTGGATAACTATTTCCAAAATAAATCACAAGCAGCTTTTCTGATCCCT HNWAATCHBDKSH
Mef2_disc1	+	12.1	7.3	DDKYTATTTTRDMH

## B.6. Power calculation

We used Genetic Power Calculator (<http://pngu.mgh.harvard.edu/~purcell/gpc/>) to estimate the effect size that our study sample size can detect with 80% power. As an example, we used rs4834703 in the *SEC24D* gene, which has 0.1 MAF and odds ratio (OR) of 1.98 from the stage II analysis. In this power calculation, we assumed 11% disease prevalence, 0.1 MAF for the marker, and the same study sample sizes (225 cases and 1830 controls). We varied the minor allele frequency of the disease locus (0.05, 0.1, 0.15) to assess the genotypic relative risk (GRR) that our study sample size can detect with 80% power. We used the same significant threshold described in the paper,  $9 \times 10^{-5}$ , for the stage II analysis. We assumed an additive model to define GRR of Aa and AA genotypes, that is,  $GRR_{Aa} = x$  and  $GRR_{AA} = 2x$ , where  $x$  is equivalent to the OR for the minor allele. If the marker tested was in complete linkage disequilibrium ( $D' = 1$ ) with the disease locus, we found that our sample size has approximately 80% power to detect a GRR = 2.6 for a rare disease locus (MAF = 0.05) and GRR = 1.8 for a more common disease locus (MAF = 0.1 and 0.15). The effect sizes become slightly higher when  $D'$  is assumed at 0.8 between disease locus and marker (**Supplemental Table S8**). The OR for rs4834703 in the *SEC24D* gene in our study was 1.97, which is consistent with the estimate here. Although somewhat controversial, current evidence supports joint 2-stage analysis designs over replication analyses in GWAS, based on increased statistical power of joint analyses,<sup>5,6</sup> which formed the rationale for our study design.

**Supplemental Table S8.** GRR estimates that our dataset can detect a given disease locus MAF at approximately 80% power when marker MAF = 0.1, sample size = 225 cases and 1830 controls, and disease prevalence = 11%.

D'	Disease locus MAF	Odds Ratio	Power
1	0.05	2.6	0.8
	0.1	1.8	0.84
	0.15	1.75	0.81
0.8	0.05	3.1	0.8
	0.1	2.15	0.84
	0.15	2	0.82

## B.7. Supplemental Table S9. Details of the top 521 SNPs identified in discovery dataset

CHR	SNP	BP	GENE SYMBOL	Minor allele	Minor allele frequency	Odds ratio	95% CI Lower Limit	95% CI Upper Limit	P-value
8	RS2044061	19723503	INTS10   LPL	G	0.3117	2.004	1.499	2.765	0.06
1	RS669197	20093341	DNMT3   CAMSAP1L1	A	0.1296	2.368	1.631	3.438	5.90E-06
1	RS12756886	200840467	CAMSAP1L1   GPR25	G	0.1215	2.342	1.612	3.404	6.12E-06
3	RS6788848	103028245	LOC102287800   ALCAM	G	0.237	1.905	1.473	2.370	8.15E-06
1	RS12039387	210819848	HHAT	A	0.05196	3.218	1.925	5.302	8.27E-06
1	RS12742404	200811765	CAMSAP1L1	G	0.1204	2.338	1.609	3.397	8.44E-06
6	RS3861449	148300251	SAMD5   SASH1	A	0.2655	1.965	1.467	2.686	8.77E-06
15	RS894157	90168108	C15orf42	G	0.1012	2.333	1.604	3.394	9.42E-06
8	RS2235118	2027154	MYOM2	C	0.1319	2.184	1.536	3.107	1.38E-05
1	RS2292066	200826769	CAMSAP1L1	G	0.1279	2.282	1.569	3.318	1.57E-05
4	RS4689485	6578487	MAN2B2	A	0.1806	2.054	1.479	2.851	1.71E-05
5	RS7271080	31973116	PDZD2	G	0.04521	3.173	1.868	5.391	1.94E-05
6	RS9382274	53877181	LRRCL1   C6orf142	A	0.07399	2.601	1.673	4.044	2.20E-05
3	RS1038517	59949140	FHIT	A	0.0898	2.477	1.622	3.782	2.68E-05
5	RS331706	124890054	ZNF608   GRAMD3	A	0.1478	2.128	1.495	3.027	2.71E-05
4	RS4834703	119691624	SEC24D	A	0.09379	2.271	1.544	3.342	3.13E-05
4	RS4302525	6552201	PPP2R2C   MAN2B2	A	0.1457	2.039	1.458	2.853	3.18E-05
13	RS9547679	31402440	RFPAP	A	0.07362	2.63	1.662	4.172	3.63E-05
1	RS12723891	21744334	ESRRG	G	0.1103	2.128	1.479	3.056	4.62E-05
19	RS3475752	48339300	CRX	G	0.0411	1.844	1.373	2.476	4.84E-05
22	RS138195	46151880	ATXN10	G	0.371	1.819	1.362	2.429	5.04E-05
6	RS2876669	148216298	SAMD5   SASH1	A	0.2328	1.891	1.389	2.573	5.12E-05
4	RS4631029	21796070	KCNIP4   NCRNA00099	G	0.09885	2.214	1.507	3.253	5.14E-05
20	RS8067635	49698104	MULTIPLE_GENES.3755.100128358	A	0.2801	1.903	1.393	2.6	5.24E-05
16	RS12920403	19756059	IQCC	G	0.1235	2.109	1.464	3.036	6.05E-05
6	RS9405142	1632299	GMD5	G	0.01484	5.575	2.4	12.96	6.46E-05
9	RS12115781	112672877	MULTIPLE_GENES.445815.114299	C	0.08401	2.359	1.545	3.601	6.97E-05
9	RS7042036	119766699	ASTN2	G	0.3168	1.81	1.351	2.425	7.13E-05
11	RS11668905	48348363	CRX   SULT2A1	G	0.3984	1.803	1.347	2.414	7.43E-05
7	RS10270288	104210910	LHFPL3	A	0.04825	3.011	1.743	5.2	7.76E-05
14	RS10140464	49210639	MDGA2   RPS29	G	0.198	1.894	1.38	2.6	7.82E-05
6	RS9352851	81392952	BCKDHB   FAM6A	A	0.3728	1.787	1.34	2.384	7.82E-05
7	RS10953524	106618074	PKNOX3   PRRAR2B	G	0.499	0.5472	0.4056	0.7881	7.86E-05
21	RS928973	43253371	PRDM15	A	0.278	0.4756	0.3287	0.6889	8.05E-05
7	RS2295145	43302195	GLB	A	0.302	1.763	1.33	2.337	8.10E-05
8	RS6558870	19797375	INTS10   LPL	B	0.3934	1.8	1.344	2.412	8.11E-05
1	RS12122147	14838630	TNKS3	G	0.1004	2.181	1.48	3.214	8.14E-05
9	RS457417	4855514	RCL1	C	0.1306	2.027	1.426	2.883	8.27E-05
15	RS11638941	39481950	LOC100289563   C15orf54	G	0.1424	2.008	1.418	2.843	8.47E-05
7	RS2058894	9726791	ACN9   TAC1	A	0.0368	3.17	1.783	5.636	8.52E-05
17	RS11077582	69911104	LOC124865   SOX9	A	0.06309	2.456	1.568	3.845	8.62E-05
8	RS13254568	11514144	BLK   GATA4	A	0.1732	1.978	1.406	2.783	8.91E-05
20	RS2425810	44890910	CDH21   SLC35C2	A	0.3924	1.787	1.335	2.391	9.38E-05
10	RS3847355	17125020	COL13A1   H2AFY2	A	0.442	1.789	1.336	2.396	9.57E-05
5	RS10078649	19877533	GFPT2   CNOT6	A	0.09818	2.174	1.471	3.212	9.80E-05
21	RS4276100	43275896	LOC102882321   PRDM15	G	0.2652	1.823	1.348	2.467	9.91E-05
2	RS11686987	107128885	RGPD3   LOC544604	A	0.03038	3.33	1.817	6.105	9.97E-05
16	RS8055711	7040933	ANR1	A	0.2881	1.825	1.348	2.47	1.00E-04
1	RS4653374	78442014	SZBP1   HREG3G	A	0.1353	2.076	1.436	3.002	0.0001033
19	RS7280398	57155195	ZNF71	G	0.4855	1.756	1.321	2.335	0.0001076
6	RS9391640	91829005	BCKDHB   FAM6A	C	0.3013	1.793	1.333	2.412	0.0001188
10	RS2885524	12565147	CAMK1D	A	0.2465	0.5135	0.3662	0.7201	0.0001112
14	RS17112396	42307496	LRFN5   F50B	A	0.01316	6.11	2.436	15.32	0.0001143
8	RS7839240	39746386	ADAM2   IDO1	G	0.3988	1.763	1.322	2.353	0.0001152
4	RS2890099	156432368	LOC100287564   GUCY1A3	A	0.1191	2.059	1.426	2.974	0.0001162
2	RS4951964	31300544	GALNT14	A	0.02767	3.535	1.86	6.719	0.0001165
14	RS1242558	83235421	SELL1   FLRT2	A	0.2912	1.785	1.329	2.398	0.0001186
15	RS12913680	90989150	LOC283671   C15orf42	A	0.1093	2.144	1.452	3.164	0.0001236
2	RS2894595	22737862	KIAA1486   IRS1	C	0.2895	1.77	1.322	2.37	0.0001245
4	RS1398835	21849857	NCRNA00099	A	0.09987	2.12	1.444	3.133	0.0001262
9	RS7035935	112706482	PALM2	C	0.06748	2.47	1.555	3.923	0.0001278
2	RS11686949	31039930	GALNT14	A	0.028	3.505	1.845	6.66	0.0001284
7	RS6461168	2107759	MAD1L1	G	0.2756	1.766	1.318	2.365	0.0001368
13	RS6663501	3740845	RFXAP   SMAD9	G	0.2257	1.827	1.34	2.491	0.0001385
12	RS11111722	104104227	STR2	A	0.05162	2.752	1.634	4.633	0.0001398
1	RS11685519	107122121	SGP3   LOC644604	A	0.03138	3.156	1.746	5.702	0.0001408
7	RS4349858	21981033	CDC41	A	0.391	1.715	1.299	2.254	0.0001422
21	RS807531	43275783	LOC100288232   PRDM15	A	0.2392	0.5185	0.3697	0.7273	0.0001424
5	RS716886	168645723	SLT3	G	0.4356	1.741	1.308	2.317	0.0001427
5	RS6556621	124899579	ZNF608   GRAMD3	A	0.2375	1.858	1.35	2.556	0.0001429
1	RS1183044	209255814	PLXNA2   LOC642587	A	0.4922	1.744	1.309	2.323	0.0001446
7	RS4148085	7727101	RPA3	C	0.4214	1.747	1.309	2.33	0.0001501
5	RS10447192	8986731	LOC100128382   SEMA5A	A	0.4069	0.5487	0.4022	0.7486	0.0001528
2	RS858940	50945699	NRXN1	A	0.3836	1.743	1.307	2.324	0.0001535
7	RS10263415	7724805	LOC729852   RPA3	A	0.4244	1.755	1.312	2.349	0.0001554
10	RS17452064	11242471	CUGBP2	C	0.1088	2.059	1.416	2.995	0.0001571
15	RS8041127	90135196	C15orf42	A	0.1043	2.118	1.435	3.128	0.0001596
6	RS6456676	2630468	LRRCL16A	C	0.01181	6.973	2.543	19.12	0.0001614
7	RS3778973	2151178	MAD1L1	A	0.208	1.809	1.329	2.462	0.0001653
13	RS7996663	37435150	SMAD9	G	0.07456	2.47	1.542	3.954	0.000167
8	RS1008641	39754780	ADAM2   IDO1	A	0.4035	1.738	1.303	2.318	0.0001693
1	RS1678949	9766898	LOC100128096   DRD5	A	0.1926	1.848	1.342	2.546	0.0001704
6	RS2201702	4696717	OPR1B	G	0.09865	2.161	1.446	3.221	0.0001718
11	RS554341	128856761	FLI1   KCN11	G	0.1334	1.946	1.374	2.754	0.0001746
20	RS7508966	40396739	CHD5   PTPRT	G	0.08603	2.294	1.487	3.539	0.0001775
2	RS1284035	19778072	C10orf112	A	0.04453	2.7	1.606	4.538	0.0001773
7	RS7802845	111723488	DOCK4	G	0.07794	2.318	1.493	3.598	0.0001797
12	RS1316899	59966101	OR6C4   OR10P1	A	0.1619	1.844	1.339	2.541	0.0001813
1	RS1054444	176649181	PAPPA2	G	0.1754	0.3867	0.2352	0.6359	0.0001814
7	RS17482047	7755484	RPA3	G	0.08835	2.177	1.448	3.272	0.0001832
1	RS10913237	176630416	PAPPA2	A	0.1748	0.3866	0.2349	0.6362	0.0001846
15	RS4774964	5784873	CGNL1   GCOM1	G	0.1859	0.4038	0.2508	0.65	0.0001892
12	RS3781519	93915922	MRPL42   SOCS2	A	0.3526	0.5349	0.3851	0.7429	0.0001894
2	RS1595422	78434830	SNARH   IRS1	A	0.1326	2.03	1.4	2.943	0.0001897
7	RS28988	119648399	SEC24D	A	0.226	1.793	1.32	2.437	0.0001899
4	RS1491152	130547852	C6orf83   LOC100132483	G	0.3347	1.74	1.3	2.329	0.0001949
20	RS6022863	52566423	SUMO1P1   BCAS1	A	0.4028	0.5521	0.4038	0.7548	0.0001965
8	RS4975192	3167178	CSMD1	G	0.03914	2.825	1.634	4.863	0.0001996
15	RS17738087	39395021	CARR3	G	0.0975	2.117	1.425	3.165	0.0002022
3	RS1706187	60203584	FHIT	A	0.0987	2.476	1.539	3.964	0.0002030
1	RS6577559	9238095	GPR157   LOC727271	A	0.1231	1.985	1.382	2.	

**Supplemental Table S9. Details of the top 521 SNPs identified in discovery dataset (cont)**

CHR	SNP	BP	GENE SYMBOL	Minor allele	Minor allele frequency	Odds ratio	95% CI Lower Limit	95% CI Upper Limit	P-value
2	RS1356799	140567666	LOC647012   LRP1B	C	0.1977	0.439	0.2783	0.6226	0.0004021
2	RS8770667	71873579	PKNOX2   RYR8	A	0.2903	1.686	1.262	2.251	0.0004067
2	RS6759163	78384746	SMARH1   REG3G	A	0.3252	1.706	1.269	2.295	0.0004101
4	RS11730104	4862927	STX19   LOC100289434	C	0.4136	1.665	1.255	2.209	0.0004125
6	RS1097194	115361857	CSDM3   TRPS1	G	0.4895	0.5859	0.4355	0.7883	0.0004131
20	RS8032661	44733811	NCOD5   CD40	G	0.2208	0.4692	0.3083	0.7142	0.0004147
20	RS8064024	52546889	SMAD1   BCAS1	G	0.4265	1.682	1.26	2.244	0.0004162
11	RS7926320	13782568	FAR1   SPON1	A	0.388	1.664	1.254	2.207	0.0004164
15	RS8043317	27751786	GABRG3	A	0.05466	2.493	1.501	4.141	0.000418
17	RS1126642	42989063	GFAP	A	0.03552	2.741	1.565	4.8	0.0004211
10	RS317499	109995284	LOC100128304   LOC645318	A	0.3357	0.5558	0.4009	0.7706	0.0004257
15	RS4777990	93018587	C15orf32	G	0.2817	1.715	1.27	2.316	0.0004304
10	RS10495786	33594529	LTPB1	G	0.1073	1.974	1.352	2.884	0.0004312
2	RS10200850	240234901	HDAC4	A	0.0652	2.22	1.424	3.462	0.0004344
3	RS9868354	108840289	MORC1   LOC100288721	G	0.02901	3.265	1.689	6.313	0.0004352
2	RS1922351	35300334	MYADM1   LOC100288911	G	0.3924	1.681	1.259	2.246	0.0004369
16	RS2396417	71356135	FTSJD1   CALB2	G	0.1265	1.927	1.337	2.777	0.0004381
20	RS2002845	71693838	THSD5	C	0.2156	1.771	1.288	2.437	0.000441
2	RS886281	56507299	COD3A	G	0.3252	1.662	1.252	2.208	0.0004457
23	RS12559251	90342188	LOC100289789   PABPC5	C	0.175	2.884	1.409	5.738	0.0004462
16	RS1424106	79216793	WWOX	A	0.4686	0.5839	0.424	0.7884	0.0004463
7	RS17533946	155347161	GALNT13   KCNJ3	A	0.2236	0.4806	0.3192	0.7236	0.000449
2	RS12220134	97129606	SORBS1	A	0.06174	2.421	1.477	3.966	0.0004499
2	RS1689880	220267737	MORPEL2   LOC100288941	A	0.02126	4.044	1.853	8.828	0.0004507
15	RS1922353	35302429	MYADM1   LOC100289111	C	0.418	1.689	1.26	2.264	0.0004518
21	RS2830247	27848998	CYR11	G	0.07625	2.105	1.388	3.193	0.0004527
9	RS7038625	16125443	C9orf3   BNC2	C	0.02193	3.692	1.778	7.666	0.0004596
2	RS2868714	44886189	CH22   SLC35C2	G	0.4879	1.676	1.255	2.237	0.0004617
13	RS9516888	97931709	MBNL2	A	0.4308	1.645	1.245	2.174	0.0004621
3	RS3932353	3925728	LOC100130652   LOC727894	A	0.277	0.5138	0.3538	0.7461	0.0004668
9	RS2503351	19182893	ADFP   LOC100288002	G	0.1694	1.826	1.303	2.558	0.0004689
19	RS1046940	17187518	MYO9B	C	0.1276	0.3353	0.1817	0.6185	0.0004691
13	RS1286943	38356247	TRPC4	G	0.2549	0.5119	0.3517	0.745	0.0004698
2	RS238632	9247782	MBO21   ASAP2	A	0.1694	0.3992	0.2386	0.6679	0.0004703
7	RS2158499	88558769	C7orf62   ZNF804B	A	0.4163	0.5763	0.4231	0.7849	0.000472
7	RS12766986	33350611	PTRM1   LOC100287172	G	0.1842	1.764	1.263	2.424	0.0004726
13	RS9491347	97930890	MBNL2	A	0.4372	1.641	1.243	2.167	0.0004732
6	RS910470	145525157	OST1   MAP3K7IP2	A	0.06515	2.367	1.46	3.836	0.0004738
7	RS2160138	7755797	RPA3	G	0.4565	1.676	1.255	2.239	0.0004741
2	RS1367241	74509618	TRHDE   LOC525889	C	0.4821	0.5933	0.4408	0.7952	0.0004749
12	RS929020	4797110	LOC100289402   FAM19A5	A	0.17	1.836	1.306	2.583	0.0004774
20	RS2425835	44901836	CH22   SLC35C2	G	0.4337	1.673	1.253	2.234	0.0004801
9	RS11143833	71433741	PIPK3B	A	0.01757	3.784	1.793	7.987	0.0004811
27	RS7284093	51121521	SHANK3	A	0.1492	1.876	1.318	2.671	0.000482
18	RS2564500	57230260	CBE1	G	0.3822	1.668	1.252	2.224	0.0004825
3	RS212020	59988905	FHIT	A	0.09615	2.096	1.383	3.176	0.0004825
6	RS3869129	31410649	MICA   HCP5	A	0.2142	1.757	1.28	2.411	0.0004847
15	RS1520015	37429504	MYO2   TMCO5A	A	0.2085	0.4596	0.2969	0.7114	0.0004863
6	RS17800315	150765510	IDO1   PLEKHG1	A	0.2419	1.709	1.265	2.309	0.0004875
6	RS3899823	31410597	MICA   HCP5	A	0.2146	1.757	1.28	2.412	0.0004887
6	RS11757015	150765316	IDO1   PLEKHG1	A	0.2421	1.708	1.264	2.309	0.0004914
7	RS2829076	716509	NIN2J   LOC100049716	G	0.2301	1.738	1.274	2.372	0.0004928
15	RS8030720	90143567	C15orf42	A	0.1005	2.016	1.359	2.99	0.0004954
12	RS4489787	48811010	ZNF641   ANP2D2	G	0.1162	0.3285	0.1756	0.6147	0.0004978
12	RS2329193	145525157	OST1   MAP3K7IP2	A	0.1775	1.788	1.291	2.49	0.0004986
7	RS1983838	44781896	CD40   CDH22	A	0.4126	0.5742	0.4201	0.7848	0.0005009
12	RS1289709	100056208	CDC85C	A	0.368	1.676	1.253	2.243	0.0005036
15	RS6576617	27035375	GABRG3   GABRA5	G	0.1053	2.004	1.354	2.965	0.0005056
18	RS4797173	466351	COLEC12	A	0.2517	1.707	1.263	2.308	0.0005061
15	RS1032725	32641200	BICD1   FGD4	G	0.3109	1.676	1.253	2.242	0.0005065
3	RS2194938	139731000	CLSTN2	A	0.1955	1.764	1.281	2.43	0.0005077
13	RS1694747	17671171	LOC390298   RERGL	A	0.08632	2.06	1.37	3.095	0.0005083
13	RS12497400	59986922	FHIT	G	0.1193	0.3111	0.161	0.6012	0.0005136
18	RS4797604	1213560	BCL6   LOC339929	G	0.1215	2.024	1.359	3.012	0.0005148
3	RS755653	18796668	SOCS7   ARHGAP23	A	0.2831	1.69	1.257	2.272	0.0005167
17	RS7502216	36612948	BCL6   ARHGAP23	A	0.3826	0.5652	0.4095	0.7801	0.0005191
13	RS11888120	29322384	C2orf71   CLP4	A	0.2456	1.707	1.262	2.309	0.0005198
2	RS2390165	166059919	SON3A	A	0.448	1.673	1.251	2.238	0.0005199
15	RS10041897	169893751	KCNMB1   KCNIP1	A	0.225	0.4793	0.3164	0.7261	0.0005201
20	RS3092167	44922717	CH22   SLC35C2	A	0.4578	1.646	1.242	2.182	0.0005235
18	RS3148415	10471732	LOC100289932   APCDD1	A	0.1144	0.2917	0.1453	0.5953	0.0005263
5	RS38691322	169897153	KCNMB1   KCNIP1	A	0.1781	0.4204	0.2575	0.6862	0.0005278
7	RS11710268	37361023	ELMO1	C	0.2196	0.4803	0.3173	0.7272	0.0005287
6	RS2223451	150767547	IDO1   PLEKHG1	A	0.2422	1.701	1.259	2.266	0.0005304
15	RS2425856	44911954	CH22   SLC35C2	A	0.4416	1.641	1.24	2.171	0.0005317
4	RS1438217	118039852	BICD1   LOC100289855	A	0.4335	1.652	1.243	2.194	0.0005318
12	RS1071958	32638162	TAC1   FGD4	C	0.3107	1.667	1.248	2.226	0.0005321
7	RS2058883	97283118	ACHN1   TAC1	A	0.1113	1.882	1.316	2.691	0.0005331
3	RS7626013	59961159	FHIT	G	0.1076	2.046	1.364	3.069	0.0005428
19	RS1972384	110210248	RAD23B   KLF4	A	0.1113	1.977	1.343	2.91	0.0005493
15	RS2840848	41998391	TM3C1   MEX3B	G	0.0105	7.914	2.448	25.58	0.0005494
6	RS476235	160622637	LOC100289162   SLC22A2	A	0.3428	1.65	1.242	2.193	0.0005521
6	RS1885487	7668923	SNRNPA4   BNP6	G	0.3222	1.71	1.261	2.318	0.0005527
1	RS12061205	176554721	PAPP2A	A	0.1515	0.3932	0.2315	0.6681	0.0005568
1	RS10494201	118252257	FAM68C   LOC100131261	A	0.3151	1.658	1.244	2.209	0.0005574
7	RS1992136	109777361	FOXN1   MYO1H	G	0.1103	0.3186	0.1664	0.6102	0.0005604
17	RS10486908	62860532	POLA1   SEMA5E	A	0.08903	2.398	1.459	3.942	0.0005634
2	RS6744657	155012898	GALNT13	A	0.237	0.4809	0.3276	0.7357	0.0005662
12	RS1091433	105377559	C15orf75   NUAK1	A	0.225	0.4811	0.3172	0.7294	0.0005682
3	RS9898107	60040105	FHIT	G	0.07996	2.157	1.393	3.34	0.0005682
9	RS11103417	137494787	RXRAL1   COL5A1	G	0.2436	0.5026	0.3398	0.7432	0.0005683
12	RS2196716	118054429	TM3C1   MEX3B	C	0.4764	0.5955	0.4434	0.7997	0.0005697
15	RS1433835	26412976	LOC100128714   GABRR3	G	0.1292	1.931	1.328	2.808	0.0005763
21	RS4919983	43301781	PRDM15   CCND2	A	0.3155	0.5512	0.3926	0.7737	0.0005765
1	RS12067235	205281255	NUAK2	A	0.2213	0.4798	0.3158	0.7291	0.0005813
8	RS6989983	115289224	CSDM3   TRPS1	A	0.4265	1.649	1.24	2.193	0.0005824
1	RS1552237	87045760	EXO1   LOC100289756	A	0.2854	1.672	1.247	2.241	0.0005854
9	RS10738231	98453680	PXCH1   MED13	A	0.4281	0.5842	0.43	0.7936	0.0005855
6	RS4767252	15187724	TBK1   MED13L	A	0.33	1.67	1.247	2.237	0.0

### Supplemental Table S9. Details of the top 521 SNPs identified in discovery dataset (cont)

CHR	SNP	BP	GENE SYMBOL	Minor allele	Minor allele frequency	Odds ratio	95% CI Lower Limit	95% CI Upper Limit	P-value
12	RS11046362	22460338	STR5A1	A	0.1046	2.003	1.336	3.001	0.000784
7	RS2204779	118438184	ANKRD7   LOC100287273	G	0.01919	4.926	1.946	12.47	0.0007853
8	RS1606891	115206234	CSMD3   TRPS1	A	0.4463	1.827	1.225	2.16	0.0007896
13	RS12268128	125646967	AKCS   TMEM132B	A	0.2449	0.5034	0.3375	0.751	0.0007898
4	RS7666244	65170415	SRD5A2L2	A	0.1859	0.4634	0.2959	0.7255	0.0007708
2	RS6547192	78434082	SVHR1   REG3G	A	0.1373	1.89	1.304	2.739	0.0007725
2	RS6432964	149898664	LYPD8	G	0.3654	0.5723	0.4133	0.7924	0.0007749
8	RS167069	115423282	CSMD3   TRPS1	G	0.4848	0.6037	0.4497	0.8102	0.0007753
11	RS10283337	1319724	LOC401442   DLGAP2	G	0.4052	1.625	1.224	2.157	0.0007815
4	RS7676913	118043203	TRAM1L1   LOC100288956	C	0.4706	0.6035	0.4495	0.8104	0.0007854
1	RS493631	153143048	SPRR2G   LELP1	A	0.1195	1.968	1.325	2.921	0.0007874
14	RS787854	94606179	IFI2L2   PPP4R4	A	0.2057	1.746	1.261	2.418	0.0007884
11	RS10894162	129781016	PRDM10	A	0.02092	3.344	1.652	6.767	0.0007912
5	RS1154758	162716850	GABRG2   CCGN1	G	0.4443	0.5973	0.4421	0.8071	0.0007932
10	RS7914288	71739556	COL13A1   H2AFY2	G	0.389	1.629	1.225	2.167	0.0007956
17	RS7219555	59740122	NACA2   BRP1	C	0.3151	1.636	1.227	2.181	0.0007979
12	RS10783915	59001589	XRCOC8BP1   LRIG3	G	0.332	0.5723	0.413	0.793	0.000798
5	RS951087	13328289	CTNND2   DNAH5	A	0.1107	1.971	1.325	2.931	0.0008055
13	RS9510573	23600990	LOC646201   SGGG	A	0.1889	1.746	1.26	2.419	0.0008068
14	RS3865845	96729728	BOKR1	A	0.37	1.639	1.228	2.189	0.0008088
1	RS6676889	205645614	PKNXA2   LOC642587	G	0.3036	0.5569	0.3952	0.7844	0.0008115
6	RS9283918	53926867	C6orf142	A	0.05904	2.267	1.404	3.661	0.0008121
6	RS9296737	53926716	C6orf142	G	0.05904	2.267	1.404	3.661	0.0008121
3	RS9841113	116455714	LOC281941   IGSF11	A	0.4339	1.62	1.222	2.149	0.0008144
5	RS1023617	172740329	NKX2-5   STC2	A	0.3128	1.66	1.234	2.235	0.0008162
3	RS4076927	46730749	ALS2C	G	0.3171	0.55	0.3875	0.7807	0.0008215
8	RS10091115	62684067	LOC100287835   NKAIN3	C	0.3381	0.5715	0.4117	0.7934	0.0008288
12	RS2364227	93883510	MRPL2	G	0.303	0.5568	0.3939	0.7844	0.0008315
21	RS2832279	30613466	C2orf109	A	0.3323	0.5744	0.415	0.7951	0.0008317
4	RS12508492	112696927	LOC729065   C4orf32	G	0.05331	2.324	1.417	3.81	0.0008328
6	RS6940801	169656667	THBS2   LOC100289536	G	0.1498	1.779	1.269	2.493	0.0008332
3	RS17485052	138638081	PK3CB   FOXL2	A	0.1991	1.75	1.26	2.43	0.0008338
12	RS10746042	106111254	C12orf75   NUAK1	G	0.2399	1.695	1.244	2.311	0.0008398
22	RS138154	46107105	ATXN10	G	0.2319	1.673	1.237	2.263	0.0008421
1	RS12120640	74821837	TNNI3K	G	0.1205	1.86	1.292	2.678	0.0008424
20	RS2425817	44895286	CDH22   SLC35C2	A	0.4329	1.633	1.225	2.179	0.0008438
7	RS4730197	106446900	FLJ36303   PK3CG	C	0.1323	0.3697	0.2061	0.6631	0.0008448
6	RS2817457	158943434	NOX3   ARH1B	A	0.4774	1.648	1.229	2.21	0.0008462
1	RS3006993	114570444	OLFM1L3   SYT6	A	0.2696	1.671	1.236	2.258	0.0008466
11	RS7128466	120491438	ARHGFEF12   GRK4	A	0.1437	0.4015	0.2349	0.6863	0.0008499
11	RS11025673	20663967	SLC6A5	G	0.3812	1.6	1.214	2.109	0.000851
3	RS1523759	77604242	ROBO2	G	0.1711	0.4267	0.2596	0.6709	0.0008541
12	RS10746041	106108279	C12orf75   NUAK1	G	0.2264	1.711	1.248	2.347	0.0008554
6	RS4895999	134147153	MGC34034	G	0.3805	1.614	1.218	2.139	0.0008575
3	RS10804937	103308760	LOC100287880   JALCAM	A	0.3184	1.624	1.221	2.16	0.0008578
13	RS9557697	101950392	NALCN	G	0.03036	2.92	1.555	5.484	0.0008589
10	RS10826503	29010588	BAMBI   LOC729601	A	0.3866	1.636	1.225	2.185	0.0008601
10	RS619030	11206281	CUGBP2	A	0.2328	1.712	1.248	2.349	0.0008633
18	RS151472	3447871	TGIF1	A	0.2908	1.652	1.229	2.219	0.0008653
1	RS476093	181787259	CACNA1E   ZNF648	C	0.2446	1.683	1.229	2.285	0.0008663
1	RS12130076	240918105	GREM2   LOC645939	G	0.1238	0.3612	0.1993	0.6577	0.0008678
2	RS2169089	5088617	AJAP1   LOC100287877	A	0.2328	0.5191	0.3529	0.7635	0.0008679
20	RS6032678	44772795	CD40   CDH22	A	0.4514	1.631	1.223	2.176	0.000871
12	RS4766019	3089354	TEAD4	A	0.123	0.3318	0.1733	0.6353	0.0008719
2	RS16965278	18734072	KOANS1   RDH14	A	0.2635	1.684	1.239	2.288	0.0008739
3	RS11633368	108946466	C3orf186   DPPA2	A	0.3219	1.621	1.22	2.155	0.0008751
7	RS11971933	111710331	DOCK4	G	0.09515	2.053	1.344	3.135	0.0008756
18	RS7506330	9177894	ANKRD12	G	0.4774	0.6034	0.4481	0.8125	0.0008765
6	RS9442693	72386001	C6orf155   RIMS1	A	0.05027	2.582	1.476	4.514	0.0008798
5	RS31036	146615260	STK32A	C	0.3286	1.644	1.227	2.203	0.0008802
7	RS914080	97271508	ACN9   TAC1	G	0.2939	1.643	1.226	2.201	0.0008811
2	RS10163733	135071570	MOAT5	A	0.1772	1.773	1.265	2.484	0.0008825
18	RS4369696	55334295	ATP9B1	A	0.2713	0.5341	0.3691	0.773	0.0008836
18	RS2345	75279459	GALR1   LOC100132713	G	0.06883	2.148	1.368	3.372	0.0008951
3	RS4974500	134109630	AMOTL2   ANAPC13	G	0.4943	0.6023	0.4466	0.8124	0.0008961
3	RS1979784	183203034	MCF2L2   KLHL6	A	0.4757	1.643	1.226	2.202	0.0008968
4	RS12511494	113770535	ANK2	A	0.141	1.859	1.289	2.682	0.0009018
6	RS2474880	63460047	KHDRBS2   LOC100128610	A	0.4325	1.638	1.224	2.192	0.0009037
11	RS11636337	70044354	LOC145837   C15orf50	G	0.251	0.5284	0.3625	0.7704	0.0009116
15	RS1827955	13996686	SPON1	G	0.2611	0.529	0.3631	0.7707	0.000912
9	RS16933086	36215581	GNE	A	0.2016	1.685	1.238	2.293	0.0009121
8	RS12547514	55806439	LOC100287651   XKR4	A	0.4172	1.638	1.224	2.194	0.0009135
7	RS13237260	7779091	RPA3   LOC729852	A	0.2415	1.665	1.232	2.252	0.000918
13	RS9532893	39394277	FREM2	A	0.4673	1.626	1.22	2.168	0.0009189
3	RS12619691	35306866	MYADM1   LOC100288911	A	0.3937	1.628	1.22	2.172	0.0009197
3	RS6766938	67150665	KBTBD8   SUGL2	A	0.2142	1.721	1.248	2.373	0.0009197
11	RS1852757	13967892	SPON1	G	0.1866	0.4711	0.3018	0.7353	0.0009207
9	RS7846713	8079286	C9orf123   PTPRD	A	0.2375	1.7	1.242	2.327	0.0009219
5	RS457638	80359968	RASGEF2	G	0.1867	0.468	0.2986	0.7333	0.0009227
19	RS9917042	14484473	CD97	G	0.3212	1.623	1.219	2.162	0.0009241
8	RS1277088	19309945	CSGALNACT1	A	0.3126	0.5837	0.4015	0.7913	0.0009254
6	RS5570569	148829305	SASH1	G	0.3333	0.5748	0.4141	0.7977	0.0009283
15	RS1783427	39503508	LOC100289653   C15orf54	C	0.1835	1.766	1.261	2.472	0.0009291
14	RS11003306	55645842	PCDH15	A	0.02092	4.64	1.87	11.51	0.0009301
10	RS1197382	81146776	C14orf145	G	0.08974	0.2693	0.1238	0.5856	0.0009328
7	RS3800895	2125942	MAD1L1	A	0.2743	1.636	1.222	2.19	0.0009334
10	RS7905027	124114432	BTBD16   PLEKHA1	G	0.3932	0.5897	0.4313	0.8063	0.0009347
2	RS6748969	175424127	GPR155   WIPF1	G	0.4906	0.6052	0.4496	0.8148	0.0009351
9	RS10814369	36292975	GNE   LOC646993	A	0.192	1.714	1.246	2.359	0.0009351
11	RS12793784	26700112	SLC5A12	A	0.1208	1.926	1.306	2.84	0.0009361
16	RS6564372	73324074	LOC100288121   LOC401859	A	0.4986	0.6197	0.4668	0.8228	0.0009375
2	RS7559847	222068646	SLCAA3   EPHA4	A	0.385	1.639	1.223	2.197	0.0009419
3	RS9790156	139814577	CLSTN2	A	0.1002	1.978	1.32	2.964	0.0009425
3	RS1925421	39250964	LOC400750   RRAAG	A	0.2567	1.645	1.225	2.21	0.0009447
23	RS10521479	55563383	LOC644693   FOXR2	A	0.1163	2.228	1.386	3.582	0.0009464
5	RS7446493	6974432	POLS   LOC442132	G	0.1029	1.905	1.3	2.791	0.0009471
1	RS3907155	10626262	LOC642337   LOC126987	G	0.4926	1.628	1.219	2.173	0.0009488
2	RS4588165	35326722	MYADM1   LOC100288911	A	0.414	1.631	1.22	2.18	0.0009507
5	RS2401793	13332878	CTNND2   DNAH5	C	0.1123	1.962	1.313	2.	

### C. SUPPLEMENTAL REFERENCES

1. Price AL, Patterson NJ, Plenge RM, Weinblatt ME, Shadick NA, Reich D. Principal components analysis corrects for stratification in genome-wide association studies. *Nat Genet.* 2006;38:904-909
2. Torkamani A, Topol EJ, Schork NJ. Pathway analysis of seven common diseases assessed by genome-wide association. *Genomics.* 2008;92:265-272
3. Liu KY, Muehlschlegel JD, Perry TE, Fox AA, Collard CD, Body SC, Shernan SK. Common genetic variants on chromosome 9p21 predict perioperative myocardial injury after coronary artery bypass graft surgery. *J Thorac Cardiovasc Surg.* 2010;139:483-488, 488 e481-482
4. Muehlschlegel JD, Liu KY, Perry TE, Fox AA, Collard CD, Shernan SK, Body SC. Chromosome 9p21 variant predicts mortality after coronary artery bypass graft surgery. *Circulation.* 2010;122:S60-65
5. Kraft P. Efficient two-stage genome-wide association designs based on false positive report probabilities. *Pac Symp Biocomput.* 2006:523-534
6. Zuo Y, Zou G, Wang J, Zhao H, Liang H. Optimal two-stage design for case-control association analysis incorporating genotyping errors. *Ann Hum Genet.* 2008;72:375-387